Energy and AI 21 (2025) 100585

Contents lists available at ScienceDirect

Energy and AI

journal homepage: www.elsevier.com/locate/egyai

Towards a smarter battery management system: A critical review on deep learning-based state of charge estimation of lithium-ion batteries

Jiaqi Yao *, Julia Kowal

Department of Electrical Energy Storage Technology (EET), Technische Universität Berlin, Einsteinufer 11, 10587, Berlin, Germany

HIGHLIGHTS

- A taxonomy of SOC estimation methods and popularly used public datasets is provided.
- A walk-through of existing deep learning-based SOC estimation methods is presented.
- Frequently applied optimization strategies are included.
- Emerging trends including PINNs, MTL, few-shot and continual learning are discussed.

GRAPHICAL ABSTRACT

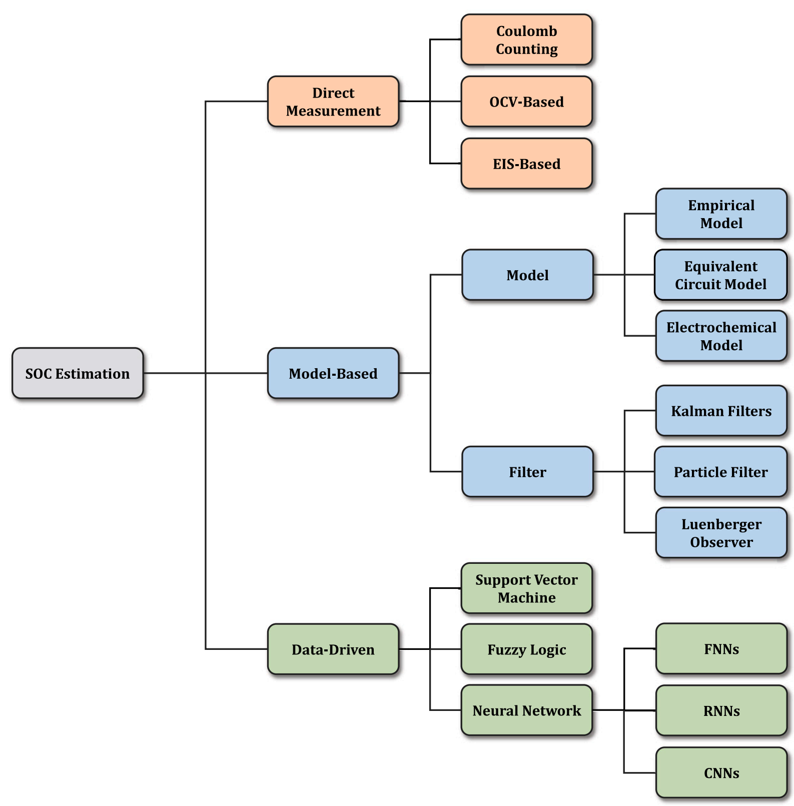

ARTICLE INFO

Keywords:
Lithium-ion batteries
Battery management systems
State of charge estimation

ABSTRACT

An accurate state of charge (SOC) estimation of lithium-ion batteries underpins a safe and optimized operation of the system. In recent years, deep learning-based SOC estimation has made significant progress. In order to provide researchers in this rapidly advancing field a comprehensive overview of the state of the art, this paper carries out a structured review on deep learning-based SOC estimation of lithium-ion batteries. A detailed

* Corresponding author.
E-mail address: jiaqi.yao@tu-berlin.de (J. Yao).

https://doi.org/10.1016/j.egyai.2025.100585
Received 2 April 2025; Received in revised form 11 July 2025; Accepted 31 July 2025
Available online 8 August 2025

Deep learning
Neural networks

taxonomy of SOC estimation approaches and popularly used public datasets is provided as an introduction to the technical background. A systematic walk-through of the existing deep learning-based SOC estimation approaches, together with the frequently applied optimization strategies, is presented, where we also appeal for a standardized evaluation protocol in this field. As highlight, the current trends and emerging perspectives are pointed out and discussed in detail, including physics-informed neural networks (PINNs), multi-task learning (MTL), few-shot learning, and continual learning. We believe this work could not only provide the researchers and practitioners new to this topic with a clear and detailed manual to start with, but also point out the emerging perspectives for further cutting-edge studies towards a smarter battery management system.

1. Introduction

With the increasing social awareness of environmental protection, the transition to broader adoption of renewable energy is accelerating. As an electrical energy storage, lithium-ion batteries have been outstanding in the market worldwide with their high energy density and power density [1–3], with their application scenarios spanning across portable electronic devices [4,5], electric vehicles [6–8], and battery energy storage systems [9–11]. In most applications, the so-called battery management system (BMS) is utilized to ensure safe and optimized usage of the battery system [12]. Basic operational data, such as the terminal voltage, current, and temperature, is measured and monitored by the BMS to ensure that the battery system runs in a safe operating window [13]. Based on the measurement data, the BMS further carries out more advanced functionalities like state estimation [14], cell balancing [15], and thermal management [16]. As one of the key internal states of the battery system, the state of charge (SOC) describes the amount of remaining usable capacity of a battery. The SOC at some time t is defined as:

$$SOC_t = \frac{Q_t}{C_{ref}} \tag{1}$$

where Q_t and C_{ref} stand for the remaining quantity of charge and the reference capacity, respectively, at time t. SOC is often defined in the range $[0, 1]$ where an SOC of 100% means the battery is fully charged, and an SOC of 0% means the battery is depleted. An accurate determination of SOC is crucial for the usage of lithium-ion batteries:

- It is the basis for the BMS to avoid dangerous operations like overcharge and overdischarge [17]. Cycling the battery outside the safety range could lead to catastrophic consequences, including the decomposition of the electrolyte, thermal runaway, permanent damage to the electrodes, causing drastic degradation of the cells, and potential safety hazards. A reliable SOC determination enables the BMS to stop the cycling in time, thus ensuring a safety operation window for the lithium-ion batteries.
- It provides information on how much energy remains available in the system for an efficient usage of the battery [18]. By getting the accurate information on the remaining energy, the system is enabled to adjust the operating strategies dynamically, thus ensuring the optimal endurance and efficiency while maintaining the required performance, mitigating possible capacity waste due to conservative operation.
- It offers real-time feedback to the users for an optimized driving behavior planning [19]. Based on the real-time monitoring of SOC, accurate remaining mileage estimates and action recommendations are made available to the drivers. The drivers could then make their decisions based on these objective evaluations as well as their own driving preferences and expectations for an optimized driving behavior planning case-by-case.

However, SOC has to be estimated as it cannot be measured directly. Furthermore, the SOC of lithium-ion batteries is dependent on various factors, including the ambient temperature [20], current intensity [21], and aging state [22]. Therefore, advanced algorithms that are able to take the various influencing factors into consideration must be applied for the task of SOC estimation of lithium-ion batteries. In general, SOC estimation algorithms can be classified into three basic categories [23]: direct measurement, model-based, and data-driven. Through the years, a tremendous number of different kinds of SOC estimation algorithms have been developed, as well as several review articles on this topic. In Ref. [24], the authors sorted different types of SOC estimation methods, with a highlight on model-based and data-driven methods. Similar topics are discussed in Ref. [14] as well, with an emphasis on the application scenario of electric vehicles. In Ref. [25], the authors covered a review of machine learning-based SOC estimation algorithms, where traditional machine learning approaches and old-fashioned neural networks were of bigger focus. However, as we all know, the research field of deep learning has been making drastic progress in recent years. The advances in deep learning models and algorithms have brought great benefits to the task of SOC estimation as well. Although some previous review articles have tried to cover the recent trends by then [26–28], the rapid growth of deep learning and deep learning-based SOC estimation is hard to capture in a timely manner. Therefore, in order to provide researchers in this field a comprehensive overview of the state of the art, this paper carries out a structured review on the existing deep learning-based approaches for SOC estimation and the current emerging perspectives in the research field. The main contribution of this paper is as follows:

1. A comprehensive introduction to the technical background is provided, including traditional SOC estimation approaches and the premise of data-driven approaches — data acquisition.
2. A systematic walk-through of the existing deep learning-based SOC estimation approaches for lithium-ion batteries is presented.
3. The current trends of deep learning-based SOC estimation are discussed in detail, pointing out the emerging perspectives of the research topics.

The rest of the paper is structured as follows: Section 2 introduces the technical background, including traditional SOC estimation approaches and data acquisition for data-driven approaches. Section 3 describes the existing deep learning-based SOC estimation approaches for lithium-ion batteries systematically. Section 4 discusses the current trends and emerging perspectives of the research field. Finally, Section 5 sums this review paper up.

2. Technical background

Fig. 1 showcases the basic classification of SOC estimation methods for lithium-ion batteries. Although many old-fashioned shallow neural networks are generally not considered part of deep learning, for this work, we treat the use of neural networks as roughly equivalent to deep learning, since shallow neural networks tend to be rarely mentioned nowadays.

2.1. Traditional SOC estimation methods

2.1.1. Direct measurement methods

Direct measurement approaches are the most intuitive SOC estimation methods. The SOC of the lithium-ion battery is derived based on the information from the measurement data. Coulomb counting, a method often used for the calculation of ground-truth SOC values

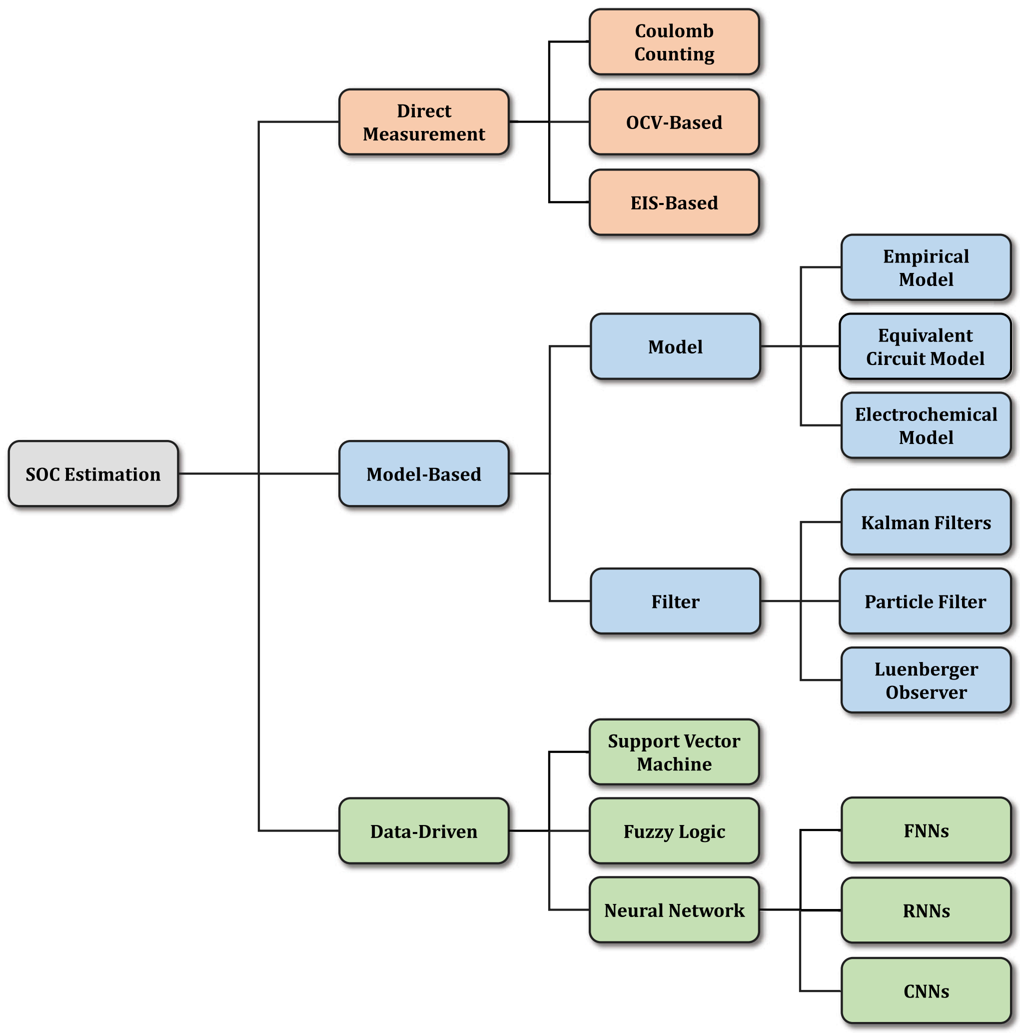

Fig. 1. General classification of SOC estimation methods for lithium-ion batteries.

in SOC estimation tasks, estimates the SOC by integrating the current flowing through the battery system over time, the equation of which is written as:

$$SOC(t_2) = SOC(t_1) + \frac{1}{C_{ref}} \int_{t_1}^{t_2} i(\tau) d\tau \tag{2}$$

Although some researchers have tried to come up with improved versions of coulomb counting [29,30], the drawback of this intuitive approach is obvious: the measurement error is prone to accumulation because of the integral operation. Furthermore, an accurate reference capacity is necessary as well. Another common direct measurement approach is the open circuit voltage (OCV)-lookup. The OCV-SOC relationship is recorded as a lookup table or polynomial in advance, which will then be used to determine the SOC when the OCV measurement is available [31,32]. Despite straightforward, OCV-based SOC estimation approaches have very limited application scenarios, as the OCV measurement is hardly accessible in real life. The electrochemical impedance spectroscopy (EIS) is a strong tool for the characterization of batteries, which can be used for SOC estimation as well. Similar to the OCV, the electrochemical impedance of a lithium-ion battery is a function of its SOC [33,34]. An impedance-SOC relationship can be therefore built up and used for the lookup of the SOC [35,36]. However, despite the fact that some BMS chip manufacturers are integrating simplified EIS functions into their chips to allow possible usage of EIS for SOC estimation [37], the application of EIS-based SOC estimation still has limited usage scenarios, as the deployment of onboard EIS measurement devices suffers from low accuracy and high cost.

2.1.2. Model-based methods

Model-based SOC estimation approaches combine the power of battery models and filtering algorithms. In a model-based SOC estimation framework, the prediction of the battery dynamics is made by the battery model, which can be empirical models [38], equivalent circuit models [39,40], and electrochemical models [41]. The prediction is then corrected by the filtering algorithm, where commonly used filtering algorithms include linear Kalman filter [42], extended Kalman filter [43,44], unscented Kalman filter [45,46], particle filter [47,48], Luenberger observer [49] and so on. Despite the fact that model-based SOC estimation approaches are robust and accurate, the implementation suffers from the demand for in-depth domain knowledge and sophisticated characterization tests for the modeling of the battery.

2.1.3. Traditional data-driven methods

Data-driven SOC estimation approaches, in general, exploit existing historical data by trying to capture the underlying patterns without the must to have a deep insight into the battery system. With the rapid development of artificial intelligence technologies and the booming amount of easily accessible data, data-driven SOC estimation approaches are increasingly gaining attention in the research field. Traditional data-driven SOC estimation methods primarily employ statistical and traditional machine learning techniques for the mapping of SOC from measurement data. For instance, as one of the most important traditional machine learning algorithms, support vector machines (SVMs) can map nonlinear relationships using the kernel trick.

With its variant support vector regression, SVMs have been applied to the task of SOC estimation as well [50,51]. However, similar to other traditional machine learning algorithms, SVMs highly depend on manual feature engineering and have limited expression ability when it comes to more complicated relationships. Another often-seen traditional machine learning approach for SOC estimation is fuzzy logic [52,53]. Instead of solely relying on data, fuzzy logic approaches are based more on expert knowledge that is encoded in the fuzzy rules in advance. This property makes fuzzy logic methods intuitive, but on the other hand also dependent on the prior knowledge from the expert, which is subjective and lacks generalization ability. Similar to SVMs, fuzzy logic SOC estimation methods are not able to deal with data with complicated underlying patterns as well.

2.2. Data acquisition

The acquisition of high-quality data is the key to the successful implementation of data-driven SOC estimation methods, which, of course, also include deep learning-based approaches. There are generally two ways for researchers to acquire such data: carrying out tests of the lithium-ion batteries by oneself, or using public datasets implemented by previous researchers.

2.2.1. Battery testing

Since the task of SOC estimation puts more emphasis on the models' performance under dynamic cycling conditions as in real life, various dynamic drive cycles are usually used for the tests [26,54]. The cycling devices apply the power profiles of the drive cycles on the batteries under testing, and the time, terminal voltage, current, and temperature measurements are recorded during the tests. Afterwards, the ground-truth SOC values can be calculated by coulomb counting with resetting at full charge or full discharge. However, such power profiles of the standard drive cycles are not easily accessible. Instead, the drive cycles are usually published in the format of velocity profiles, which have been collected and sorted by some organizations, such as The National Renewable Energy Laboratory [55]. Special approaches are needed to manually translate these velocity profiles into power profiles that can be recognized by the battery testing devices. In Ref. [56], a simple two-wheel vehicle model is utilized for the translation from velocity profiles to power profiles. Carrying out self-designed tests allows one to tailor the data to their specific needs and conditions, which further brings novelty to the research work.

2.2.2. Public datasets

An alternative to acquire the desired data for data-driven SOC estimation tasks is to use public datasets that were published by other researchers in this field. They are usually easily accessible online, which saves time and resources for the development process. In addition, using public datasets enables comparative analyses with other previous studies that used the same dataset, facilitating benchmarking and validation. Table 1 lists some selected lithium-ion battery drive cycle datasets. The public dataset from the University of Wisconsin-Madison (UW-Madison) [57] is currently most used [38,58–60]. For the dataset, the authors performed tests on a brand-new Panasonic 18 650 2.9 Ah lithium nickel cobalt aluminum (NCA) cell. The tests were conducted under five different ambient temperatures controlled by a climate chamber, including 25 °C, 10 °C, 0 °C, −10 °C, and −20 °C. At each temperature, the cell was cycled with nine drive cycles, of which four cycles were distinct standard drive cycles, and the rest five were synthesized from the distinct cycles. Using the same data synthesis approach, the authors published two similar datasets at McMaster University [61,62]. However, such data synthesis could lead to overlaps of the underlying patterns of different drive cycle samples, which further leads to overfitting of the data-driven SOC estimation models instead of gaining generalization abilities, posing a serious threat to their reliability and robustness when exposed to novel real-life cycling profiles and casts doubts on the research works whose results are based on the utilization of these datasets. To remove this problem, we have published a novel lithium-ion battery drive cycle dataset [63] recently with a detailed description of the data acquisition procedure [56]. For the dataset, three brand-new LG 21 700 lithium nickel manganese cobalt (NMC) cells with 4.93 Ah nominal capacity under the same aging state were cycled under five ambient temperatures, including 45 °C, 35 °C, 25 °C, 15 °C, and 5 °C. At each temperature, the cells were cycled with twelve distinct drive cycles with no possible overlaps in the underlying patterns. Therefore, it is ensured that the performance of SOC estimation models trained on this dataset comes from their generalization ability instead of overfitting. The dataset from Center for Advanced Life Cycle Engineering (CALCE) at the University of Maryland [64] is another commonly used public drive cycle dataset, which contains the cycling profiles of a Samsung 18 650 2 Ah NMC cell under four drive cycles, namely Dynamic Stress Test (DST), Federal Urban Driving Schedule (FUDS), Beijing Dynamic Stress Test (BJDST), US06 Supplemental Federal Test Procedure (US06), at 45 °C, 25 °C, and 0 °C, and a Wanxiang 18 650 1.1 Ah lithium iron phosphate (LFP) cell under the three cycles of DST, US06, FUDS at eight different ambient temperatures.

2.2.3. Data preprocessing

For deep learning-based SOC estimation tasks, data preprocessing is essential for the models' performance. Usually, after getting the measurement data of the voltage, current, and temperature, regardless of whether they are from public datasets or measured ourselves, the following preprocessing procedure should be considered:

1. Calculate the SOC labels of the cycling profiles. The label value is the fundamental target for the training of neural networks later, and thus must be accurately determined. Ordinary coulomb counting is often prone to accumulated error through time. Therefore, the most commonly used approach for SOC label calculation is coulomb counting with reset. At the beginning of a drive cycle, the voltage reading of the sufficiently relaxed cell can be considered as OCV and used for resetting. In most public datasets, the cells start with 100% SOC for each drive cycle, as they have been previously fully charged under the CC-CV charge protocol.
2. Resample the cycling profiles. Raw measurement data often have slightly varying sampling rates because of the hardware limitation, even though a certain constant sampling rate has been specified in the test schedule. Such nuances in the sampling rate might lead to misunderstandings of the temporal dynamics by the SOC estimation models. A common approach for data resampling is interpolation, which guarantees data uniformity while maintaining authenticity.
3. Split the dataset into three subsets: training set, validation set, and test set. The network updates its parameters based on training set data and is fine-tuned based on its performance on the validation set. Only the performance on the unseen test set should be reported to reflect the generalization ability of the model objectively. The commonly used ratio for data splitting is 6:2:2.
4. Normalize the input features. The commonly used input signals, including the voltage, current, and temperature, often have completely different ranges. In order to equalize the influence caused by the numerical range of each input feature and accelerate the training process, input features should be normalized using min–max normalization or z-score standardization. It is worth mentioning that the statistical parameters used for normalization should solely come from training set samples to avoid potential information leakage. Then use the same parameters for normalization in validation and testing.

After the preprocessing procedure, including label calculation, profile resampling, data splitting, and input normalization, the data is now ready for further model development.

Table 1
Public lithium-ion battery drive cycle datasets.

Source	Cell type	Drive cycle	Ambient Temp. [°C]
UW-Madison [57]	Panasonic 18650 2.9 Ah NCA	4 distinct, 5 synthetic	25, 10, 0, −10, −20
McMaster [61]	LG 18650 3 Ah NMC	4 distinct, 8 synthetic	40, 25, 10, 0, −10, −20
McMaster [62]	Samsung 21700 3 Ah NMC	4 distinct, 8 synthetic	40, 25, 10, 0, −10, −20
TU Berlin [63]	LG 21700 4.93 Ah NMC	12 distinct	45, 35, 25, 15, 5
CALCE [64]	Samsung 18650 2 Ah NMC	4 distinct	45, 25, 0
CALCE [64]	Wanxiang 18650 1.1 Ah LFP	3 distinct	50, 40, 30, 25, 20, 10, 0, −10

3. Existing deep learning-based approaches for SOC estimation

As mentioned before, the field of deep learning has made prosperous progress in recent years. As an advanced type of data-driven SOC estimation method, deep learning models, namely neural networks, offer tremendous advantages in capturing complex underlying patterns behind the data in various operating conditions. They are able to carry out automatic feature extraction from measurement, such as the terminal voltage, current, and temperature, and map those features into the desired SOC estimates, which makes deep learning-based SOC estimation approaches free from not only in-depth domain knowledge but also from efforts for manual feature design. Furthermore, as discussed in this section, the diverse architectures and paradigms of neural networks also offer a variety of possibilities for the advanced modeling of battery dynamics with different emphases subject to the developer. In the following part of this section, the commonly used basic architectures of neural networks for SOC estimation of lithium-ion batteries are first systematically presented, followed by the often applied optimization strategies for deep learning models used for SOC estimation. A comparative analysis of the selected research works is presented along with the usual evaluation metrics for this task.

3.1. Neural network architectures

As the center of deep learning, neural networks are able to capture complex nonlinear underlying patterns from the data. For that purpose, a variety of different architectures have been proposed for neural networks with different strengths. These network architectures process the input data in distinct ways, as some try to capture the long-term dependencies, and some focus on local features. In this section, the commonly used basic neural network architectures and the corresponding research works regarding SOC estimation of lithium-ion batteries are enumerated.

3.1.1. Feedforward neural networks

The conventional feedforward neural network (FNN), also known as multilayer perceptron (MLP), is a basic type of neural network consisting of fully connected (FC) layers with nonlinear activation functions. As shown in Fig. 2, in an FNN each neuron in the hidden layers and the output layer is connected to every neuron of the previous layer for the calculation of the weighted sum and the nonlinear activation. For a hidden layer with i neurons and j inputs, the calculation can be written in such form:

$$\begin{bmatrix} h_1 \\ \vdots \\ \vdots \\ h_i \end{bmatrix} = f(\begin{bmatrix} w_{11} & \cdots & \cdots & w_{1j} \\ \vdots & \ddots & & \vdots \\ \vdots & & \ddots & \vdots \\ w_{i1} & \cdots & \cdots & w_{ij} \end{bmatrix} \begin{bmatrix} x_1 \\ \vdots \\ \vdots \\ x_j \end{bmatrix} + \begin{bmatrix} b_1 \\ \vdots \\ \vdots \\ b_i \end{bmatrix}) \tag{3}$$

where h_i represents the output of the ith neuron, w_{ij} represents the weight parameter related to the ith neuron and the jth input, b_i represents the bias parameter of the ith neuron. f is the activation function that introduces nonlinearity into the mapping function of the neural network. Commonly used activation functions include rectified linear unit (ReLU), the sigmoid function, the hyperbolic tangent function $tanh$, and so on. Based on such a combination of weighted sum and activation function, FNNs process the information unidirectionally from the input to the output.

In the context of SOC estimation of lithium-ion batteries, FNNs are able to effectively build up the nonlinear relationship between the measurable parameters, such as the terminal voltage, current, and temperature, and the underlying SOC. In Ref. [59], the authors used a deep FNN for battery SOC estimation, which takes the voltage, temperature, average current, and average voltage at some time step as input and produces SOC as output. The average current and average voltage is calculated over some predefined precedent time steps. The proposed deep FNN was trained and tested on the UW-Madison dataset under two different ambient conditions, namely fixed ambient temperature and varying ambient temperature. In the case of fixed ambient temperatures, the model was trained and tested individually at each ambient temperature. In the case of varying ambient temperatures, the data profiles from different ambient temperatures are put together and used to train and test the model. At the fixed ambient temperature of 25 °C, the FNN was able to achieve a mean absolute error (MAE) of 1.35% on the test profile of Highway Fuel Economy Test (HWFET). When trained with multi-temperature data and tested on the HWFET profile of 25 °C, the FNN had an MAE of 1.10% instead. In Ref. [65], the authors developed a three-layer feedforward backpropagation neural network (BPNN) for estimating SOC of lithium-ion batteries, which takes current, voltage, and temperature as inputs and was additionally fine-tuned using the backtracking search algorithm (BSA). Using the CALCE NMC dataset, the proposed network was trained and tested with two drive cycles, namely DST and FUDS, at three different temperatures of 45 °C, 25 °C, and 0 °C. On the test profiles of DST, the model achieved the MAE of 0.87%, 0.59%, and 0.38% at 0 °C, 25 °C, and 45 °C, respectively. In Ref. [66], the authors proposed an improved deep neural network (DNN) for SOC estimation of lithium-ion batteries for electric vehicle applications. The proposed DNN takes the instantaneous voltage, current, and temperature readings as input and outputs the estimated SOC. The effect of the network depth on the estimation accuracy was studied as well. The proposed network was trained on the CALCE NMC dataset consisting of four drive cycles at three different temperatures of 45 °C, 25 °C, and 0 °C. The proposed DNN was found to have the best performance when having three hidden layers, which achieved an MAE of 0.093% on the test profile of DST.

Unquestionably, vanilla FNNs are simple neural networks that are intuitive and easy to implement. On the task of SOC estimation of lithium-ion batteries, FNNs are able to achieve a relatively good performance in cases where the cycling patterns are uncomplicated and the conciseness of the estimation model is of great importance. However, their architecture determines that they are not able to capture the long-term temporal dependencies in the input data unless extra feature engineering is done, like adding averaged current and voltage of some previous time steps as input in Ref. [59]. Moreover, FNNs are prone to overfitting because of their large number of parameters in the fully connected layers, which increases the memory cost as well. Therefore, FNNs are generally not considered the first choice for deep learning-based SOC estimation of lithium-ion batteries nowadays.

3.1.2. Recurrent neural networks

Recurrent Neural Networks (RNNs) are an advanced type of neural networks that are particularly designed for sequence processing. RNNs utilize recurrent connections and internal states in order to retain historical information in the information flow across time. Fig. 3 shows

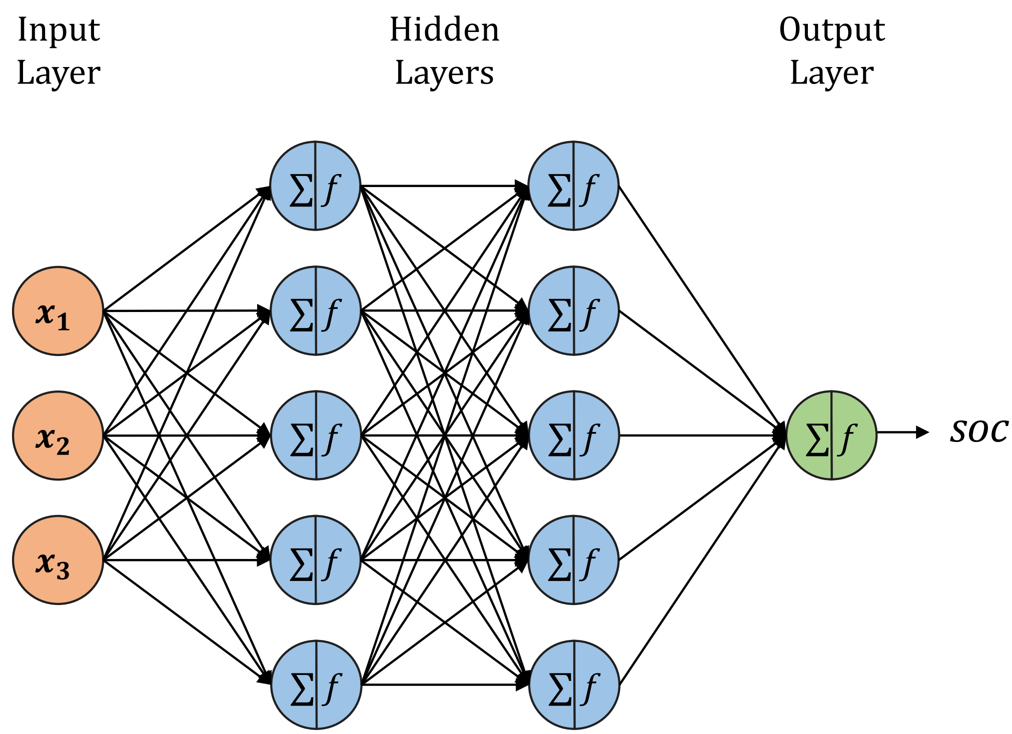

Fig. 2. An example FNN with two hidden layers.

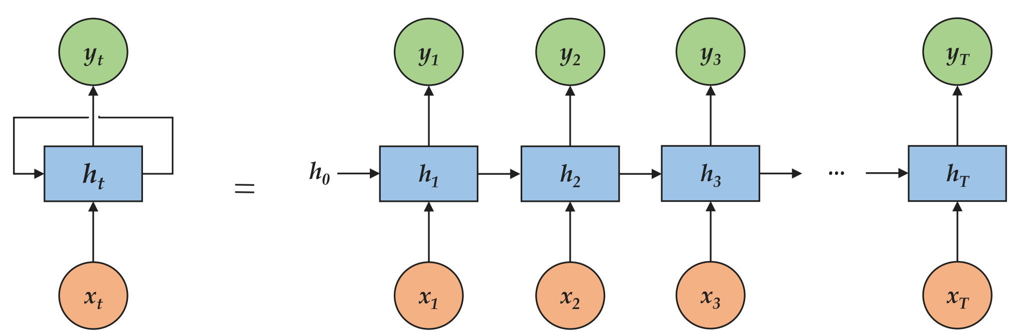

Fig. 3. Elman RNN unrolled over time.

the information flow of an Elman RNN unrolled over time, where the previous hidden state is fed back as an input. For a vanilla Elman RNN that only has one hidden layer, the hidden state $\boldsymbol{h}_t$ and the output $\boldsymbol{y}_t$ at time step t can be computed recursively as follows:

$$\boldsymbol{h}_t = f(\boldsymbol{W}_{xh}\,\boldsymbol{x}_t + \boldsymbol{W}_{hh}\,\boldsymbol{h}_{t-1} + \boldsymbol{b}_h) \tag{4}$$

$$\boldsymbol{y}_t = f(\boldsymbol{W}_{hy}\,\boldsymbol{h}_t + \boldsymbol{b}_y) \tag{5}$$

where $\boldsymbol{W}_{xh}$, $\boldsymbol{W}_{hh}$, $\boldsymbol{W}_{hy}$ are the trainable weight matrices, $\boldsymbol{b}_h$ and $\boldsymbol{b}_y$ are the trainable bias vectors. At each time step, a vanilla RNN receives two inputs, namely the input vector $\boldsymbol{x}_t$ of the current time step and the hidden state vector $\boldsymbol{h}_{t-1}$ of the previous time step.

Because of the recursive architecture of RNNs, they are widely applied for time series processing, including SOC estimation of lithium-ion batteries. In Ref. [67], the authors developed a deep RNN model for this purpose, which was fine-tuned using the firefly algorithm (FA) for the optimal hyperparameters. The model was trained and tested on the dataset consisting of a static discharge and a hybrid pulse power characterization (HPPC) test of two different types of lithium-ion cells at room temperature. On the test profile of the HPPC test, the proposed deep RNN was able to achieve an MAE of 0.512% for the NMC cell and an MAE of 0.423% for the NCA cell. In Ref. [68], the authors proposed a modified version of standard RNN, namely clockwork recurrent neural network (CWRNN). The proposed CWRNN utilizes the separated modules assigned with different clock speeds to model the long-term temporal dependencies and takes the current, voltage, and temperature measurements as input. The UW-Madison public dataset was used for this work. On the test profile of HWFET, the proposed model trained with multi-temperature data was able to achieve an MAE of 1.30% at 25 °C and an MAE of 1.67% at −10 °C.

However, vanilla RNNs suffer from the problems of vanishing gradients and exploding gradients when it comes to modeling long-term dependencies, as there is no selection mechanism in their memorization of historical information. Therefore, researchers have introduced more advanced variants. As one of the most used advanced versions of RNN, long short-term memory (LSTM) [69] introduced an extra cell state vector and a gating mechanism to control which historical information to forget and which to retain. Compared with vanilla RNNs, LSTM is more capable of capturing the long-term dependencies of the sequences and is partially immune to the problem of vanishing gradients. Fig. 4 shows the internal architecture of an LSTM unit. At each time step, three input vectors are fed into an LSTM unit, namely the input vector of the current time step $\boldsymbol{x}_t$, the cell state of the previous time step $\boldsymbol{c}_{t-1}$, and the hidden state of the previous time step $\boldsymbol{h}_{t-1}$. Two output vectors, namely the cell state $\boldsymbol{c}_t$ and the hidden state $\boldsymbol{h}_t$ of the current time step,

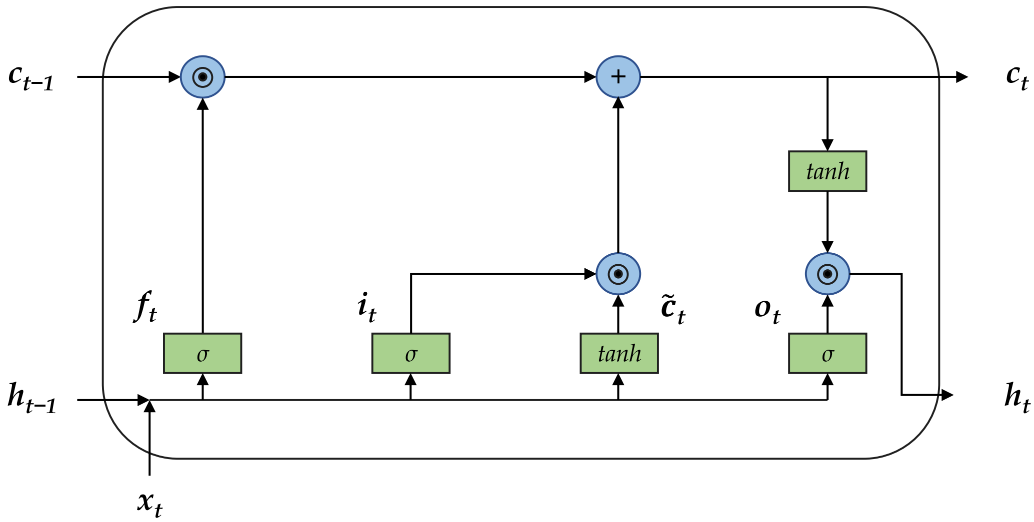

Fig. 4. LSTM unit internal architecture.

are calculated at each time step using the following mapping equations:

$$i_t = \sigma(\boldsymbol{W}_{xi}\boldsymbol{x}_t + \boldsymbol{W}_{hi}\boldsymbol{h}_{t-1} + \boldsymbol{b}_i) \tag{6}$$

$$f_t = \sigma(\boldsymbol{W}_{xf}\boldsymbol{x}_t + \boldsymbol{W}_{hf}\boldsymbol{h}_{t-1} + \boldsymbol{b}_f) \tag{7}$$

$$o_t = \sigma(\boldsymbol{W}_{xo}\boldsymbol{x}_t + \boldsymbol{W}_{ho}\boldsymbol{h}_{t-1} + \boldsymbol{b}_o) \tag{8}$$

$$\tilde{c}_t = tanh(\boldsymbol{W}_{xc}\boldsymbol{x}_t + \boldsymbol{W}_{hc}\boldsymbol{h}_{t-1} + \boldsymbol{b}_c) \tag{9}$$

$$c_t = f_t \odot c_{t-1} + i_t \odot \tilde{c}_t \tag{10}$$

$$h_t = o_t \odot tanh(c_t) \tag{11}$$

where f_t, i_t, $\tilde{c}_t$, o_t denote the vectors of the forget gate, input gate, candidate cell state, output gate, respectively. The current hidden state and the cell state are calculated by combining the previous information after forgetting and the current information after selection.

Because of the advantages of LSTM, it is widely used in deep learning-based SOC estimation of lithium-ion batteries in the research field nowadays. In Ref. [58], the authors used an LSTM network for online SOC estimation of lithium-ion batteries. At each time step, the proposed network takes the voltage, current, and temperature measurements as input. The model was trained and tested on the UW-Madison dataset under both fixed and varying ambient temperatures. The test results showed that the LSTM network was able to achieve an MAE of 1.030% averaged over two drive cycles at the fixed ambient temperature of 10 °C and an MAE of 0.774% on one mixed drive cycle at 25 °C when trained with multi-temperature data. In Ref. [70], the authors proposed a stacked LSTM network to estimate the SOC of LFP cells. The network takes the current, voltage, and temperature measurements as input and was trained and tested on a private 18 650 1.1 Ah LFP dataset consisting of DST, US06, and FUDS at room temperature. When trained with two of the three drive cycles and tested with the other one, the model achieved an MAE of 0.84% when FUDS is used as test data, an MAE of 1.08% when US06 is used as test data, and an MAE of 2.02% when DST is used as test data. In Ref. [71], the authors proposed a stacked bidirectional LSTM (Bi-LSTM) network for SOC estimation of lithium-ion batteries. The bidirectional architecture of RNNs extracts information from the input in both forward and backward directions, leading to a more comprehensive representation. The proposed network was trained and tested on the UW-Madison dataset and the CALCE NMC dataset. On the UW-Madison dataset, the model achieved an MAE of 0.73% on US06 at 25 °C when trained with multi-temperature data of 25 °C, 10 °C, and 0 °C. On the CALCE dataset, the model had an MAE of 0.59% on US06 at 25 °C. In Ref. [72], the authors proposed an LSTM network with extended input and constrained output (EI-LSTM-CO). A slow time-varying information sliding window average voltage was designed as an extra input of the network for the reduction of the estimation fluctuations. A state flow strategy was utilized for the constraint of instant changes in the output SOC for the same purpose as well. The proposed model was trained and tested on the CALCE LFP dataset at the seven temperatures above 0 °C. The proposed EI-LSTM-CO model achieved an RMSE of 0.4% on the test cycle US06 and an RMSE of 0.5% on FUDS, respectively at 25 °C. In Ref. [73], the authors proposed a bidirectional LSTM network with postprocessing for SOC estimation of lithium-ion batteries, namely Savitzky-Golay filter-based bidirectional LSTM (SG-BiLSTM). After the Bi-LSTM produces the SOC estimates, the Savitzky-Golay filter is used to smooth the curve of estimation locally. The authors developed a private dataset of 18 650 2.9 Ah NCA cells using Urban Dynamometer Driving Schedule (UDDS). The proposed SG-BiLSTM model takes the voltage and current measurements as input without considering the temperature, which outperformed conventional FNN, RNN, and Bi-LSTM with an RMSE of 1.15% on the original test set and an RMSE of 1.16% on the new test set imposed with random noise. In Ref. [74], the authors applied an LSTM network for SOC estimation using the UW-Madison dataset as well, which had an MAE of 0.66% on the synthesized cycles at 25 °C. In Ref. [75], the authors proposed a hybrid framework for SOC estimation of lithium-ion batteries, where an autoencoder that takes the voltage, current, and ambient temperature as input is used for feature extraction, and an LSTM is used for the SOC estimate regression from the latent space representation learned by the hidden layers of the autoencoder. Two cycles, namely DST and FUDS, of the CALCE NMC dataset were utilized for the work. On the test cycle DST, the proposed autoencoder-LSTM achieved an MAE of 0.6664% at 25 °C. On the test cycle FUDS, the proposed model had an MAE of 0.6312% at the same ambient temperature.

Besides LSTM, gate recurrent units (GRUs) [76] are another popularly used advanced variant of RNNs. Although LSTM is able to capture the long-term dependencies of the sequences, its training is still complicated because of the relatively large number of parameters introduced by the three gates. To improve upon that, GRUs drop the cell state and only use the hidden state $\boldsymbol{h}_t$ to transmit the information. Furthermore, GRUs rely on only two gates, namely the update gate and the reset gate, which leads to a leaner architecture and higher computational efficiency, making them more suitable for tasks that

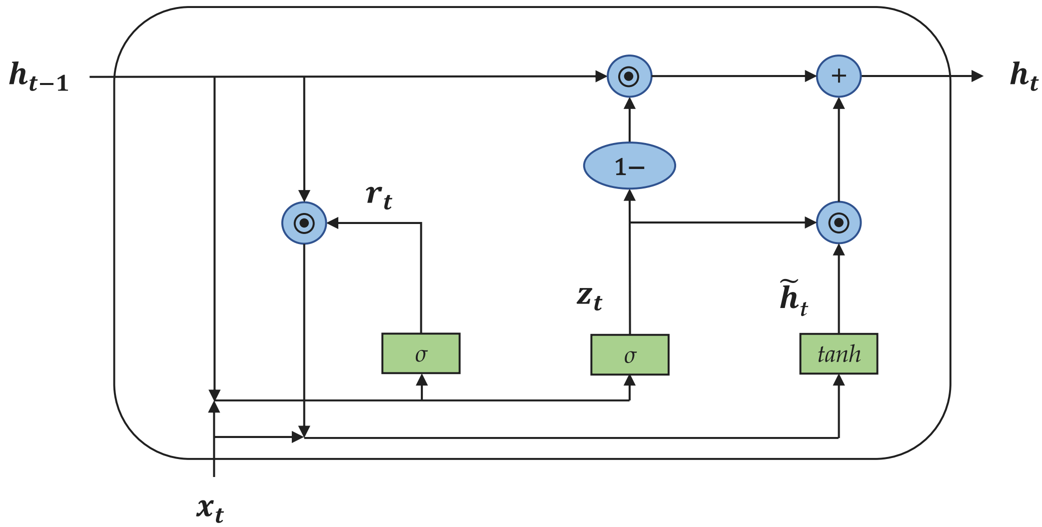

Fig. 5. GRU internal architecture.

are not very complicated and have a limited amount of data. Fig. 5 shows the internal architecture of GRUs. The mapping equations are as follows:

$$z_t = \sigma(W_z x_t + U_z h_{t-1} + b_z) \tag{12}$$

$$r_t = \sigma(W_r x_t + U_r h_{t-1} + b_r) \tag{13}$$

$$\tilde{h}_t = tanh(W_h x_t + U_h (r_t \odot h_{t-1}) + b_h) \tag{14}$$

$$h_t = (1 - z_t) \odot h_{t-1} + z_t \odot \tilde{h}_t \tag{15}$$

where z_t, r_t, $\tilde{h}_t$ are the vectors of the update gate, reset gate, and the candidate activation state, at time step t, respectively. The current hidden state is calculated by combining the weighted previous information and the selected new candidate state.

GRUs have been widely applied in the field of SOC estimation of lithium-ion batteries as well. In Ref. [77], the authors proposed a GRU network for SOC estimation that takes the current, voltage, and temperature measurements as input and outputs the SOC at each time step. Three 18 650 1.3 Ah NMC cells were put under test with two dynamic drive cycles, namely DST and FUDS, under seven ambient temperatures of 0 °C, 10 °C, 20 °C, 30 °C, 40 °C, 50 °C, and room temperature. The experiment setup of fixed ambient temperature and varying ambient temperature was utilized as well. In the case of fixed ambient temperature of room temperature, the proposed GRU model had an MAE of 0.77% on DST with 150 hidden neurons trained over 2000 epochs. In the case of varying ambient temperature, the model had an MAE of 1.65% on DST at room temperature. GRU is used in Ref. [78] as well for SOC estimation with a similar setup. But instead of using solely a private dataset, the authors utilized the UW-Madison dataset, the CALCE NMC dataset, and a self-developed high rate pulse discharge condition dataset using a 18 Ah battery. The experiments conducted on the UW-Madison dataset were divided into the two cases of fixed and varying ambient temperatures as well. The model achieved an MAE of 1.86% on US06 at the fixed ambient temperature of 25 °C. On the other hand, when trained with multi-temperature data, the model was able to achieve an MAE of 0.68% on US06 at 25 °C. In Ref. [79], the authors utilized a stacked GRU model with two hidden layers for SOC estimation of lithium-ion batteries at variable ambient temperatures. The CALCE NMC dataset was used for the development of the model in this work. The stacked GRU model was able to achieve an MAE of 0.127% on the test cycle of FUDS and an MAE of 0.091% on the test cycle of US06. In Ref. [80], the authors proposed an improved GRU network, namely GRU with activation function layers (GRU-ATL). Three activation function layers, namely a *tanh* layer, a leaky ReLU layer, and a clipped ReLU layer, were augmented into the GRU network for better accuracy. The McMaster LG dataset was utilized for the work. In the test case of varying ambient temperatures, the proposed model was able to achieve an MAE of 0.814% on the cycle UDDS and an MAE of 0.978% on the cycle US06, at 25 °C, respectively. In Ref. [81], a bidirectional GRU (Bi-GRU) network trained with the Nesterov accelerated gradient (NAG) algorithm was proposed for SOC estimation. Similar to Bi-LSTM, Bi-GRU takes the information flow from both forward and backward directions into consideration for a more comprehensive feature extraction. The NAG algorithm was utilized to reduce the oscillation during training and accelerate the process. The network takes a vector of temperature, voltage, and current as input and outputs SOC. Two public datasets were used in the study, namely the CALCE NMC dataset and the McMaster LG dataset. When trained on multi-temperature data, the model was able to achieve an MAE of 1.02% on the test cycle of FUDS of the CALCE dataset at 25 °C. On the other hand, the model had an MAE of 1.132% on the test cycle of UDDS of the McMaster dataset at 25 °C. In Ref. [82], a data-driven framework consisting of a denoising autoencoder (DAE) for feature extraction and a GRU for SOC regression was proposed for SOC estimation. The input data of the voltage, current, and temperature is fed into the DAE and deliberately corrupted with random noise, which will then be mapped into latent space representation using the encoder part and subsequently reconstructed to the original input vector by the decoder part. The features extracted by the hidden layers of the DAE will then be fed into the GRU model for the mapping of the SOC estimates. In order to verify the proposed DAE-GRU model, the authors developed a private dataset using a 18 650 3 Ah NMC cell. The cell was tested with three drive cycles, namely UDDS, HWFET, and New European Driving Cycle (NEDC) at room temperature. On the test cycle of UDDS, the model trained with NEDC had an MAE of 1.1942%, which outperformed the GRU model (1.5049% MAE) and the RNN model (1.5100% MAE).

The recursive nature of RNNs determines that they are most appropriate in cases where the accurate estimation is strongly dependent on the long-term temporal history, such as under complicated dynamic cycling conditions. With the advanced RNN architectures like LSTM and GRU, the problems of vanishing gradient when dealing with long-term dependencies have also been mitigated. Although the architecture of RNNs might seem complicated, they are actually perfect for online SOC estimation scenarios as in real life in embedded environments. As long as the RNNs are implemented in a synchronous many-to-many style, the computation at each time step only includes the mapping

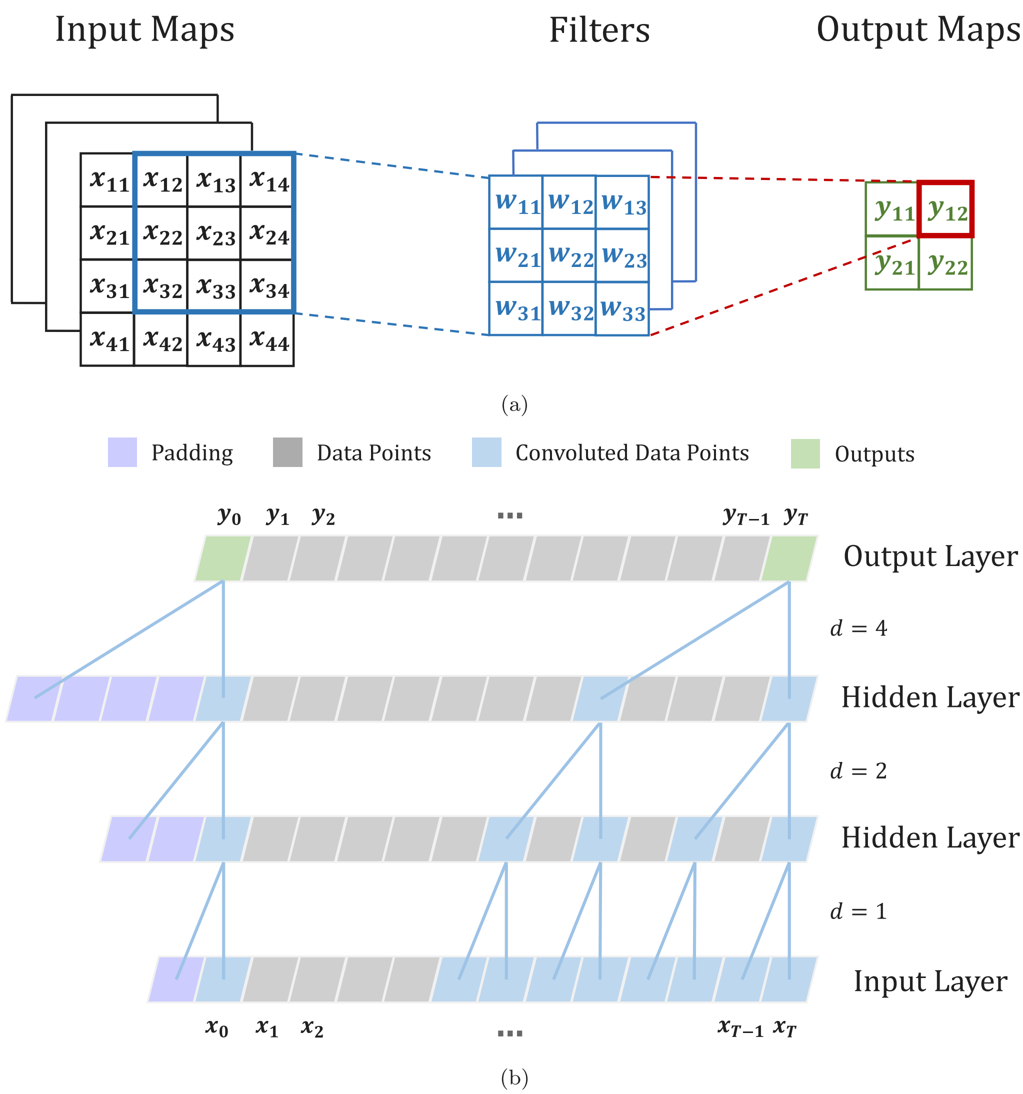

Fig. 6. CNN and TCN. (a) Mapping operation of an example CNN. (b) TCN unrolled through time.

of the previous hidden state vectors and the current input vector, leading to significantly less computational effort compared with FNNs or convolutional neural networks, where a whole input window needs to be considered for the SOC estimation at each time step. However, the training of RNNs can be notoriously hard because of the complicated gradient flow during backpropagation through time. Therefore, as mentioned in Section 3.1.1, simpler FNNs might be preferred in cases where the cycling pattern is less dynamic or the historical sequence for consideration is relatively short.

3.1.3. Convolutional neural networks

Convolutional neural networks (CNNs) are another advanced variant of neural networks that have been widely applied in the field of computer vision. Fig. 6(a) showcases the mapping operation of an example CNN. For an input feature map of size $H \times W$ with a single channel, the mapping operation using a stride of 1 can be expressed as follows:

$$y_{i,j} = \sum_{u=0}^{k-1} \sum_{v=0}^{l-1} x_{i+u,j+v} \cdot w_{u,v} \tag{16}$$

where $i = 1, 2, \ldots, H - k + 1$ and $j = 1, 2, \ldots, W - l + 1$. w is the filter of size $k \times l$.

Benefiting from the featured convolution operation, CNNs are particularly good at local feature extraction and modeling complex nonlinear relationships between the input and the output. Therefore, CNNs have been applied to the task of SOC estimation as well. In Ref. [83], a 1D CNN model was proposed by the authors for SOC estimation of electric vehicles. The model treats the input vector of voltage, current, and temperature as a 1D vector with three channels. The UW-Madison dataset and the McMaster LG dataset were utilized for the development of the model. The training was carried out in the case of varying ambient temperatures, namely the cycling profiles under different ambient conditions were used to train and test the model together. On the UW-Madison dataset, the proposed model reached an MAE of 0.71% on the test cycle US06 under the sampling rate of 10 Hz and a historical window size of 1000 without imposed noise. On the McMaster LG dataset, the model reached an MAE of 0.44% on the test cycle US06 under the same condition. In Ref. [84], a U-Net CNN model was proposed by the authors for SOC estimation of lithium-ion batteries. In addition, a symmetric padding convolution layer that mirrors the data on both ends of the sequence as padding was proposed to enhance the estimation of the boundaries. The model was trained and tested on the UW-Madison dataset using multi-temperature data. The model reached an MAE of 1.1% at 25 °C and an MAE of 0.9% at 0 °C on the test cycle US06. Extra validation was carried out to test the model's performance under changing temperatures as well. In Ref. [85], the authors proposed a CNN model that maps the features from 2D time-frequency domain spectrograms to SOC estimates contrary to other 1D CNN networks for SOC estimation. The authors utilized the SpecAugment technique to enhance the model's generalization abilities as well. The UW-Madison dataset was utilized for the model's training and testing, which was resampled to 1 Hz as preprocessing. Experiment results show that the proposed model with SpecAug outperforms the conventional models, including CNN, LSTM, CNN-LSTM, FNN, and CNN-BiGRU with an MAE of 0.52% at −20 °C and an MAE of 0.53% at 25 °C on the test set.

CNNs are particularly good at extracting spatial dependencies from the data. However, SOC estimation is about capturing temporal dependencies from the measurements. Despite the fact that some 1D CNNs have been applied for this purpose, they rely heavily on long input sliding windows in order to capture the long-term dependencies in the data. Furthermore, because of the convolution operation of CNNs, they are not suitable for online SOC estimation by design, as the mapping from the input to the output is not causal. To address the aforementioned matters, temporal convolutional networks (TCNs) [86] were introduced as a variant of CNNs especially designed for time series data processing. TCNs feature the so-called dilated causal convolution. Fig. 6(b) shows an example TCN unrolled through the time axis. Dilation is utilized in the convolution operation to expand the receptive field. A dilation factor of d means that every dth input data point is considered in the convolution operation, and the presented setup of the three dilation factors results in a total receptive field of 8. In this way, the output at each time step is able to take more input data points into consideration without increasing the number of parameters by either extending the length of the input sliding window or deepening the network. Meanwhile, an architectural padding trick is utilized in TCNs to ensure causality. A certain number of paddings are concatenated onto the beginning of each input sequence so that the output is aligned with the input with respect to the time step, i.e. the output at each time step only takes the historical input data points into consideration. Denote the input sequence with $\boldsymbol{X}$ and the filter with the kernel size k with $\boldsymbol{W}$, the dilated convolution operation C at some time step t can be defined as follows:

$$C(t) = (\boldsymbol{X} *_d \boldsymbol{W})(t) = \sum_{i=0}^{k-1} \boldsymbol{W}(\boldsymbol{i}) \cdot \boldsymbol{x}_{\boldsymbol{t-d\cdot i}} \tag{17}$$

Compared to RNNs for time series processing, TCNs have the advantage of the convolution operation of different time steps being calculated in parallel instead of one after another, which increases the training efficiency and stability significantly. Consequently, TCNs have been widely applied in SOC estimation. In Ref. [87], the authors proposed a TCN model with a transfer learning technique for SOC estimation of lithium-ion batteries. The model maps the measurements, including voltage, current, and temperature, directly into SOC estimates. The UW-Madison dataset was used to develop the model. In the case of a fixed ambient temperature of 25 °C, the model had an average MAE of 0.54% on the four mixed test cycles. While training with data from multiple temperatures, the average MAE became 0.67% on the four test cycles at 25 °C. In Ref. [88], the authors proposed a separable TCN that combines depth-wise and point-wise temporal convolution. The UW-Madison dataset was used for the work. At 25 °C, the model had an MAE of 2.56% on the test cycle of HWFET and an MAE of 0.77% on the test cycle of US06. In our previous work [56], a multi-scale data-driven framework was proposed for online SOC estimation of lithium-ion batteries. The framework utilizes a multi-scale TCN module consisting of four sub-TCNs with different lengths of receptive fields for feature extraction and a cross-scale self-attention module for feature fusion. The developed framework was tested on two different public datasets, namely the UW-Madison dataset and the TU Berlin dataset. On the UW-Madison dataset, the proposed framework achieved an MAE of 0.363% on the test cycle California Unified Cycle (LA92) at 25 °C in the case of fixed ambient temperatures. On the TU Berlin dataset, the framework achieved an MAE of 0.612% on the test cycle Port Drayage Metro Highway Cycle California (PDMHC) at 25 °C in the case of varying ambient temperatures. Test results showed that the proposed multi-scale framework outperforms conventional sequence-to-sequence models in most test cases.

CNNs are particularly suitable for cases where local feature extraction and efficient inference are required at the same time, as the convolution operation can be done in parallel. Through deliberate architecture design, CNNs can be easily made to capture short-term as well as long-term dynamics by stacking the convolutional layers or increasing the dilation factor of the convolution operation to tune the length of the receptive field [56] to our own need. Compared with RNNs, the possibility of parallel operation makes the training much less time-consuming as well. However, because the length of the receptive field is often pre-defined through the architecture design, practitioners should have some basic understanding of the time scale of the battery dynamics they are trying to capture. Compared with FNNs, CNNs are able to achieve the same length of receptive field with much fewer parameters, but usually with a larger computational cost. Therefore, FNNs might be a simplified alternative when the sequence dependency is very short and computational cost is the priority. As for online estimation scenarios like in real life, TCNs are still based on sliding windows as with FNNs, which leads to a larger memory cost in embedded systems compared with RNNs.

3.2. Optimization strategies

In the previous section, the basic neural network architectures for SOC estimation of lithium-ion batteries have been introduced in detail. However, those networks in vanilla forms need to be optimized with various add-on approaches for the full capability to deal with the dynamic data and the complex underlying patterns. Therefore, we present several optimization strategies that are often applied to neural networks for accurate SOC estimation.

3.2.1. Hyperparameter optimization for optimized performance

Deep learning models are highly sensitive to hyperparameters like the learning rate, number of neurons, and network depth. The training of the models will become extremely time-consuming and prone to local optima without well-tuned training hyperparameters. Furthermore, unstable network architectures, such as the network depth or number of neurons, will lead to underfitting or overfitting of the model. However, the hyperparameter space can be very large because of the number of tunable hyperparameters. Effective hyperparameter optimization (HPO) is, therefore, crucial in the development of deep learning models. So far, commonly used search algorithms for HPO include grid search, random search, Bayesian optimization and its variants, tree Parzen estimators (TPEs), and so on [89]. In Ref. [90], the authors utilized Bayesian optimization for the hyperparameter fine-tuning of a Bi-LSTM for SOC estimation of lithium-ion batteries. Four hyperparameters, namely the number of neurons of the hidden layer, the initial learning rate, the decay factor of the learning rate, and the maximum number of epochs, were chosen to be optimized in the work. Test results showed that the Bayes-optimized Bi-LSTM performed best compared with LSTM and Bi-LSTM. In Ref. [91], the authors utilized the TPE for the HPO of a deep Bi-GRU network for SOC estimation. The Hyperband pruning algorithm was applied as well in order to save time and resources when it comes to unpromising trials. Twelve hyperparameters were optimized using the algorithm with 50 trials in total. Test results showed that the proposed Bi-GRU with TPE achieved the lowest RMSE and MAE in the case of varying ambient temperatures on various drive cycles. In Ref. [92], the authors utilized the genetic algorithm (GA) to optimize the key parameters of a GRU network for SOC estimation. GA carries out the search for the optimal solutions by imitating natural evolution. The number of GRU layers and FC layers and their respective neurons were chosen to be optimized. The proposed approach was proven to be highly accurate and robust. In Ref. [93], the authors used the random search algorithm to optimize the important parameters of an LSTM network for SOC estimation, i.e., the look back, epoch, batch size, and learning rate. Additionally, the random forest algorithm was used to extract the important features for the estimation of SOC. Test results showed that the proposed framework achieved superior precision.

HPO strategies can be integrated with any network architecture, regardless of being FNNs, RNNs, or CNNs. For each architecture, the tunable training hyperparameters are the same, only the architecture hyperparameters vary. For example, CNNs have more unique architecture hyperparameters, such as the number of channels, kernel size, stride, and dilation factors. However, the procedure works in the same way. Applying HPO strategies is particularly useful for cases where a new model is developed from scratch or an existing model needs to be applied to a new dataset or different cycling conditions. In such cases, manually tuning the hyperparameters is highly time-consuming. With HPO strategies, optimized configurations can be found automatically with efficiency. Furthermore, HPO strategies can effectively reduce the model size and computation for balanced accuracy and cost, which is essential for deployment in embedded systems.

3.2.2. Attention mechanism for optimized temporal modeling

The task of SOC estimation requires accurate temporal modeling of the battery, capturing the complex dynamics between different features over a considerable length of history. In addition, the contribution of different input signals can vary for each time step, where a dynamic weighting method for such information is beneficial. The attention mechanism [94,95] is a machine learning technique that imitates the attention of humans, i.e. our capabilities to focus on the most important part of information when dealing with a chunk of information input. Applying the attention mechanism to neural networks enables the model to learn to capture the most important part of information while focusing less on the less important part by assigning the weight parameters to the features dynamically. In the field of time series processing, such as natural language processing, the attention mechanism has proven to be able to effectively model the input sequence taking the context into consideration after proper training. In recent years, the attention mechanism has been widely applied in the task of SOC estimation using deep learning, as the battery data is often highly dynamic time series with complex underlying patterns. In Ref. [96], the authors proposed a GRU-based encoder–decoder network with dual-stage attention for accurate estimation of SOC. A spatial attention mechanism was used in the encoder stage to extract the important features from the input data, while a temporal attention mechanism was utilized to take the correlation of the time series into consideration. Test results showed that the proposed framework was able to achieve an accurate estimation of SOC. In Ref. [97], the authors proposed a hybrid deep learning model for SOC estimation, which combines TCN, GRU, and attention mechanism. TCN and GRU were used to comprehensively extract the temporal features with long-term dependencies. The attention mechanism was used to highlight the important pieces of temporal information by assigning the weight parameters to the hidden states of the sequences. Test results showed that the proposed model was accurate and robust when estimating the SOC of different types of batteries at different ambient temperatures. In Ref. [98], the authors proposed an LSTM model with an attention mechanism for SOC estimation of lithium-ion batteries. The attention mechanism was used to construct the LSTM through the depth of time in a different way and model the long-term dependencies. In Ref. [99], the authors proposed a Bi-GRU network with squeeze-and-excitation attention and Savitzky-Golay filter as postprocessing for SOC estimation. After the temporal features were captured by the Bi-GRU, the squeeze-and-excitation attention was used to highlight the useful information through a squeezing operation and an excitation process. The proposed method has been proven effective in the SOC estimation of LFP cells. In Ref. [100], the authors proposed a framework that consists of parallel-connected self-attention and LSTM modules for SOC estimation. The multi-head self-attention was utilized in this work to directly model the long-term dependencies of the input sequences. The proposed model was trained and tested on the self-developed NCA dataset with gapped temperature data. Test results showed that the proposed model was able to deliver SOC estimation results that were accurate, robust, and practical. In Ref. [101], an attention-based encoder–decoder network was proposed for SOC estimation of lithium-ion batteries under complex ambient conditions. The encoder was constructed from a Bi-LSTM network, followed by a sequence pattern attention layer to capture the context and temporal patterns comprehensively. The generated hidden state vector was then fed into the decoder for the regression of the SOC estimates. The proposed framework was validated on the UW-Madison dataset and has showcased outstanding accuracy.

The attention mechanism can be integrated with different model architectures for the information weighting between different time steps as well as different channels. Such ways of information weighting are particularly useful for complex cycling patterns, where the batteries are cycled extremely dynamically regarding the current or ambient temperature. Models with attention mechanisms can automatically focus on those moments with drastic changes, providing robust estimation. In addition, the attention mechanism can also be utilized for feature fusion, where a variety of input information is presented, and the network has to capture the important ones at each time step dynamically. However, attention mechanisms are often computationally intensive, which should therefore be carefully deliberated in real-life applications.

3.2.3. Transfer learning for optimized training

Training is always a crux for deep learning models. For SOC estimation models, the training often requires comprehensive efforts in architecture design, hyperparameter determination, and loss monitoring, when they are developed from scratch with randomly initialized parameters. Transfer learning is a machine learning technique that aims at transferring previously learned knowledge of one domain or task into another relevant domain or task, so that the learning efficiency and generalization abilities of the model on the new task will be strengthened [102]. Transfer learning has become a common strategy in many practical applications, where neural networks are first pre-trained extensively on large datasets for the learning of generic underlying features, and then fine-tuned on the specific datasets for the tasks at hand. In the context of SOC estimation of lithium-ion batteries, the utilization of transfer learning techniques can bring great advantages as well. Lithium-ion batteries of different materials often show comparable behaviors and dynamics, resulting in datasets with similar characteristics under different operating conditions. By leveraging transfer learning for SOC estimation, pre-trained neural networks trained on some lithium-ion battery datasets that have already learned the essential underlying temporal dependencies can quickly adapt to new battery types or cycling scenarios, reducing the demands on data and improving the model's performance. In Ref. [103], the authors proposed an LSTM network for SOC estimation of lithium-ion batteries with transfer learning. Data from four different types of lithium-ion batteries was utilized in this work. Test results showed that through transfer learning, the proposed model's accuracy in SOC estimation was improved, and less training data was required. In Ref. [104], the authors proposed an LSTM model with canonical variate analysis (CVA)-based feature extraction for SOC estimation. Transfer learning was utilized for the model to learn at new temperature conditions. Test results on the UW-Madison dataset showcased that the model achieved higher estimation accuracy at new temperatures with transfer learning from the reference temperature. In Ref. [105], the authors proposed a controllable deep transfer learning network for SOC estimation, where controllable multiple domain adaptation was utilized for the knowledge transfer from historical battery data to the target battery's SOC estimation. Using adaptive regularization, negative knowledge transfer was mitigated. The controllability and convergence of the transfer learning were offered by the proposed network as well. Test results showed that the proposed network was superior to existing deep learning and transfer learning benchmarks. In Ref. [106], eight different transfer learning approaches were examined on four different models, including

LSTM, GRU, Bi-LSTM, and Bi-GRU. Three datasets were used in the study, namely the CALCE NMC dataset, the McMaster LG dataset, and a private dataset developed by the authors. Test results showed that the hybrid transfer learning technique and adaptive hidden states transfer learning technique outperformed the rest in terms of both accuracy and computational time.

Transfer learning is a universal technique for the training of deep learning models. In practice, no matter if it is FNN, RNN, or CNN, a backbone for feature extraction can be first trained on large-scale public datasets, and then the estimation heads can be fine-tuned on the target battery. This technique provides great potential value for fast model development. Furthermore, transfer learning can be used for online updating of SOC estimation models. The model can be continuously fine-tuned through the operation of the battery systems, keeping an accurate SOC estimation while saving labeling costs.

3.2.4. Hybrid model for optimized robustness

As a safety-critical task, SOC estimation often requires strong robustness against noise. In addition, BMSs are sensitive to latency. Therefore, the optimization method often has to be both trustworthy and lightweight. As different SOC estimation approaches have their own unique advantages, hybrid models can often benefit from the combination of strengths and achieve better overall performance when dealing with complicated tasks. In the context of SOC estimation, data-driven models are intelligent and powerful in terms of capturing temporal features but suffer from uncertainties as they are black-box models without sufficient explainability, while model-based approaches are often robust with the underlying battery models but have limited capabilities in modeling highly dynamic cycling cases. Therefore, data-driven models have often been integrated with model-based approaches to enhance the accuracy and stability in recent researches. In Ref. [107], the authors proposed a hybrid SOC estimation framework that combines an extended Kalman filter (EKF) with LSTM optimized with particle swarm optimization. The battery model's prediction serves as the prior estimated SOC and the output of the LSTM model serves as the measurement, whereas EKF is utilized to harness both for an enhanced SOC estimation. Validation results showed that the proposed hybrid framework achieved excellent accuracy and robustness. In Ref. [108], the authors proposed a hybrid framework for SOC estimation of LFP cells, where an LSTM network was utilized to capture the underlying battery behaviors and an unscented Kalman filter (UKF) to eliminate the noise and estimation errors. Similarly, the output of the LSTM network is also considered as the measured SOC, which is used to correct the battery model's prediction, namely the coulomb counting model. Experimental results demonstrated that the proposed hybrid method delivered satisfying estimation results under varying temperatures and temperatures where no training data was provided. In Ref. [109], the authors proposed a hybrid framework for SOC estimation, also combining EKF and LSTM, but with a different workflow. In their work, the EKF is used to produce the updated state estimates and the Kalman gain, which will then be fed into the LSTM network together with the operational measurements as input. The final SOC estimate is produced by the LSTM network. This layout has proven to deliver higher accuracy than using EKF or LSTM alone. In Ref. [110], the authors proposed a hybrid framework consisting of CNN, Bi-GRU, and adaptive UKF (AUKF), namely CNN-BiGRU-AUKF, for SOC estimation of lithium-ion batteries. Like in Ref. [108], the proposed framework utilizes CNN-BiGRU to generate the preliminary SOC estimates, which are considered measurement and subsequently corrected using AUKF and a coulomb counting model. Specifically, the model's scalability was validated in the work as well. In Ref. [111], a generic hybrid fusion framework integrating deep learning models and Kalman filters for SOC estimation of lithium-ion batteries was proposed. The basic idea of the proposed fusion framework is to use a fusion method to combine the estimation of the deep learning model and the Kalman filter with battery models. In their work, a spatial–temporal awareness model based on the encoder–decoder architecture with spatial and temporal attention mechanisms was proposed as the deep learning model. Experiments were conducted on three different adaptive nonlinear Kalman filters using a simplified electrochemical model and seven different fusion methods, where test results showed that the adaptive cubature Kalman filter and kernel ridge regression appeared to be the best options.

As discussed, there are different ways to combine neural networks with nonlinear filters for hybrid SOC estimation models. When it comes to real-life applications, such hybrid models provide strong robustness against noise, which is particularly suitable for usage scenarios where the measuring precision is suboptimal. Furthermore, introducing nonlinear filters into the neural networks brings more interpretability and reliability to the SOC estimation models, making them easier to certify, just like adding an additional lock to the black box.

3.3. Comparative analysis

SOC estimation is a regression task, where the performance can be evaluated in different aspects. Commonly adopted evaluation metrics include MAE, RMSE, and the coefficient of determination R^2, which are usually defined as follows:

$$MAE(\boldsymbol{y}, \hat{\boldsymbol{y}}) = \frac{1}{n}\sum_{i=1}^{n} |y_i - \hat{y}_i| \tag{18}$$

$$RMSE(\boldsymbol{y}, \hat{\boldsymbol{y}}) = \sqrt{\frac{1}{n}\sum_{i=1}^{n} (y_i - \hat{y}_i)^2} \tag{19}$$

$$R^2(\boldsymbol{y}, \hat{\boldsymbol{y}}) = 1 - \frac{\sum_{i=1}^{n} (y_i - \hat{y}_i)^2}{\sum_{i=1}^{n} (y_i - \bar{y})^2} \tag{20}$$

where $\boldsymbol{y}$ is the ground-truth sequence, $\hat{\boldsymbol{y}}$ is the estimated sequence, and $\bar{y}$ is the mean of $\boldsymbol{y}$. MAE reflects the overall estimation error simply and intuitively, which represents the average distance between the ground truth and the estimates. RMSE is more sensitive to outliers, as the error is magnified through the square operation. Therefore, RMSE partially represents the level of fluctuation of the estimation and is often higher than MAE. R^2 reflects the model's performance based on its explanation ability of the variance in the data, which is also a common metric to describe a regression model's fitting performance.

Table 2 summarizes the aforementioned different deep learning models for SOC estimation of lithium-ion batteries. For each model, we not only showcase the performance under the evaluation metric MAE, but also the utilized dataset, the specific test case, and the controlled environmental condition. This is because the performance of the proposed models of each work cannot be directly compared with each other quantitatively, as the utilized cell types and experimental setups differ from work to work, despite the fact that we have made great efforts to document the reported results under cycling conditions that are as comparable as possible. Therefore, Table 2 should be treated as an overview of previously developed possibilities of deep learning-based SOC estimation approaches. From this summary, some conclusions can be drawn, which would further guide practitioners through implementation by providing insights into the models' strengths and weaknesses.

First, the fundamental architecture of models. As the most basic type of neural network, FNNs have rarely been applied to the task of SOC estimation, with mediocre performance compared with other models, which is the same for vanilla RNNs. Advanced variants of RNNs, e.g. LSTM and GRU, appear to be the most frequently applied models for SOC estimation of lithium-ion batteries because of their inherent capabilities in time series processing and improvements for the training process. Stacked LSTM and GRU are commonly seen in research works, where multiple LSTM or GRU layers are used for temporal feature extraction. On the one hand, the models gain stronger

Table 2
Comparison of selected deep learning models' performance on SOC estimation of lithium-ion batteries.

Model	Dataset	Performance	Test case	Temp.
Deep FNN [59]	UW-Madison dataset	1.35% MAE 1.10% MAE	HWFET HWFET	Fixed, 25 °C Varying, 25 °C
Feedforward BPNN with BSA [65]	CALCE NMC dataset	0.87% MAE 0.59% MAE 0.38% MAE	DST DST DST	0 °C 25 °C 45 °C
DNN [66]	CALCE NMC dataset	0.093% MAE	DST	0, 25, 45 °C
Deep RNN with FA [67]	Private 18650 2.6 Ah NMC Private 18650 3.2 Ah NCA	0.512% MAE 0.423% MAE	HPPC HPPC	Room temp. Room temp.
CWRNN [68]	UW-Madison dataset	1.30% MAE 1.67% MAE	HWFET HWFET	Varying, 25 °C Varying, −10 °C
LSTM [58]	UW-Madison dataset	1.030% MAE 0.774% MAE	Two drive cycles One mixed drive cycle	Fixed, 10 °C Varying, 25 °C
Stacked LSTM [70]	Private 18650 1.1 Ah LFP	0.84% MAE 1.08% MAE 2.02% MAE	FUDS US06 DST	Room temp. Room temp. Room temp.
Stacked Bi-LSTM [71]	UW-Madison dataset CALCE NMC dataset	0.73% MAE 0.59% MAE	US06 US06	Varying, 25 °C 25 °C
EI-LSTM-CO [72]	CALCE LFP dataset	0.4% RMSE 0.5% RMSE	US06 FUDS	25 °C 25 °C
SG-BiLSTM [73]	Private 18650 2.9 Ah NCA dataset	1.15% RMSE 1.16% RMSE	UDDS UDDS with noise	Room temp. Room temp.
LSTM [74]	UW-Madison dataset	0.66% MAE	Synthesized cycles	25 °C
Autoencoder-LSTM [75]	CALCE NMC dataset	0.6664% MAE 0.6312% MAE	DST FUDS	25 °C 25 °C
GRU [77]	Private 18650 1.3 Ah NMC	0.77% MAE 1.65% MAE	DST DST	Fixed, room temp. Varying, room temp.
GRU [78]	UW-Madison dataset	1.86% MAE 0.68% MAE	US06 US06	Fixed, 25 °C Varying, 25 °C
Stacked GRU [79]	CALCE NMC dataset	0.127% MAE 0.091% MAE	FUDS US06	0, 25, 45 °C 0, 25, 45 °C
GRU-ATL [80]	McMaster LG dataset	0.814% MAE 0.978% MAE	UDDS US06	Varying, 25 °C Varying, 25 °C
NAG-based Bi-GRU [81]	CALCE NMC dataset McMaster LG dataset	1.02% MAE 1.132% MAE	FUDS UDDS	Varying, 25 °C 25 °C
DAE-GRU [82]	Private 18650 3 Ah NMC	1.1942% MAE	UDDS	Room temp.
1D CNN [83]	UW-Madison dataset McMaster LG dataset	0.71% MAE 0.44% MAE	US06 US06	Varying, −20, −10, 0, 10, 25 °C Varying, −20, −10, 0, 10, 25 °C
CNN with U-Net [84]	UW-Madison dataset	1.1% MAE 0.9% MAE	US06 US06	Varying, 25 °C Varying, 0 °C
CNN with 2D time-frequency domain spectrograms [85]	UW-Madison dataset	0.52% MAE 0.53% MAE	30% of the dataset 30% of the dataset	Fixed, −20 °C Fixed, 25 °C
TCN [87]	UW-Madison dataset	0.54% MAE 0.67% MAE	Four mixed drive cycles Four mixed drive cycles	Fixed, 25 °C Varying, 25 °C
Separable TCN [88]	UW-Madison dataset	2.56% MAE 0.77% MAE	HWFET US06	25 °C 25 °C
Multi-scale TCN [56]	UW-Madison dataset TU Berlin dataset	0.363% MAE 0.612% MAE	LA92 PDMHC	Fixed, 25 °C Varying, 25 °C

capabilities in representation learning by deepening the network depth, which helps the models capture complicated underlying patterns in the given data. On the other hand, stacking RNN layers causes great increases in computational cost. Therefore, the depth of the RNNs must be carefully chosen, taking the complexity of the cycling scenarios and the requirements for efficiency into consideration. Bidirectional RNNs, such as Bi-LSTM and Bi-GRU, have also been frequently applied in research works due to their ability to extract temporal features in both forward and backward directions. Similar to stacked RNNs, such implementation increases the real-time computational cost, which is a major drawback for real-life usage scenarios. Therefore, bidirectional RNNs might be more suitable for offline SOC estimation in the research context. While in real-life applications, often the computational constraints are the bottleneck that should be prioritized. Compared with RNNs, CNNs have been less frequently used for SOC estimation, possibly because they are not intrinsically designed for time series processing and temporal feature extraction. However, as a freshly proposed variant of CNN, TCNs are particularly designed for synchronous sequence-to-sequence time series processing, i.e. online SOC estimation, which is important for the real-time evaluation of energy storage systems. Generally speaking, online SOC estimation is more meaningful than offline estimation when it comes to real-life applications. However, many works that focus on better feature extraction have implemented their estimation model in an offline estimation style, which might have limited potential in practice.

Second, the selection of datasets. Most research works chose to use public datasets for convenience, which also facilitated the horizontal comparison with other approaches. Among all works, the UW-Madison dataset has been most frequently used. Although it covers a wide range of ambient conditions from −20 °C to 25 °C, the existence of the synthesized cycles could jeopardize the training of the models with information leakage, such that the performance no longer represents

Table 3
Summary of the optimization methods of deep learning models for SOC estimation.

Strategy	Method	Objective
Hyperparameter optimization	Bi-LSTM with Bayesian optimization [90]	Selection of the number of neurons of the hidden layer, initial learning rate, decline factor of the learning rate, maximum number of epochs
	Bi-GRU with TPE [91]	Selection of the number of hidden layers, number of GRU cells, learning rate, optimizer, batch size, output activation, patience, maximum epochs, loss function, error metric, input lag window, normalization range
	GRU with GA [92]	Selection of the number of GRU and FC layers and their respective neurons
	LSTM with random search	Selection of the look back, epoch, batch size, and learning rate
Attention mechanism	GRU-based encoder–decoder model with dual-stage attention mechanism [96]	Feature extraction from the input data and modeling of the temporal correlation
	TCN-GRU-Attention Network [97]	To highlight important temporal information of the sequence
	LSTN with attention mechanism [98]	To construct the LSTM through the depth of time differently and model the long-term dependencies
	Bi-GRU with squeeze-and-excitation attention and Savitzky-Golay filter [99]	To boost key information
	Self-attention-LSTM [100]	To directly model the long-term dependencies of the input sequences
	Bi-LSTM based encoder–decoder with attention mechanism [101]	To capture the context and temporal patterns comprehensively
Transfer learning	LSTM with transfer learning [103]	To improve estimation accuracy and reduce the amount of training data on new battery types
	CVA-based LSTM with transfer learning [104]	To improve estimation accuracy at new temperatures
	Controllable deep transfer learning network [105]	To mitigate the negative knowledge transfer and guarantee controllability and convergence of transfer learning
	Eight different transfer learning techniques on four different models [106]	To improve accuracy and reduce training time
Hybrid model	EKF-LSTM [107]	To harness both the prior prediction of the battery model and the measurement produced by the LSTM
	LSTM-UKF [108]	To use UKF to eliminate noises and estimation errors in the LSTM's estimation
	EKF-LSTM [109]	To use EKF for extra input features of the LSTM network for accurate estimation
	CNN-BiGRU-AUKF [110]	To use AUKF to filter out the SOC estimates of the CNN-BiGRU network
	A generic fusion framework for deep learning models and Kalman filters [111]	To enhance estimation accuracy and robustness in comparison of single models

the generalization ability fairly. As a result, many of the performance reported in the research works where this dataset is used may actually reflect the models' ability to memorize the overlapping patterns rather than truly capturing the underlying electrochemical dynamics. When applied to real-life novel drive cycles, the models could possibly have a significant decrease in estimation performance. Consequently, the confidence in the research works' claims about the superiority of particular network architectures or optimization strategies is undermined. The practical guidance that these studies provide BMS developers must be carefully reviewed case-by-case, as practitioners focus mainly on real-life applications where the applied estimation model must be robust across diverse unseen operating scenarios. Therefore, in order to provide researchers and developers with a more objective validation environment, we developed the TU Berlin dataset that only covers distinct drive cycles with diverse cycling patterns [56].

Third, ambient conditions. Different ambient condition setups have been applied to the development of the models as well, such as fixed ambient temperatures, varying ambient temperatures (multiple temperatures), or constantly changing ambient temperatures, among which the testing case of varying ambient temperatures fits better to reality, as the temperature change is often quasi-static, but the loaded estimation model is required to function in different ambient conditions. Most works utilized MAE as one of the evaluation metrics. However, each research work had a different way of data splitting and experimental setup, which baffles the direct comparison between different approaches.

Table 3 is a summary of the mentioned optimization methods of deep learning models for SOC estimation, including hyperparameter optimization (HPO), attention mechanism, transfer learning, and hybrid models. Deep learning models are highly volatile because of the huge number of tunable hyperparameters and the nature of black-box models, which makes HPO essential to their performance. A systematic HPO is necessary to bring out the potential of deep learning models on SOC estimation of lithium-ion batteries. In the selected research works, a variety of HPO approaches have been applied to deep learning models for the selection of diverse hyperparameters of training and architectures, achieving satisfying results. The attention mechanism is dedicated to better feature extraction, with a wide choice of different variants. However, as aforementioned, such attempts in fine-grained feature extraction often lead to significantly higher computational costs and are thus not suitable for real-life applications. The developer must carefully consider whether the addition of attention mechanisms is worth the cost of efficiency based on the specific tasks. Similar to HPO, transfer learning is another optimization method for deep learning models, which is easy to implement in offline training and does

Table 4
Model architecture comparison matrix for SOC estimation.

Criterion	FNNs	RNNs	CNNs
Temporal modeling	Short-window mapping	Long-term dependencies	Moderate history via dilation
Latency	Very low	High (window-based)/low (synchronous many-to-many)	Moderate
Computational cost	Low	High (window-based)/very low (synchronous many-to-many)	Moderate
Parameter count	Large	Small	Moderate
Onboard bottleneck	Memory cost	Latency, computational cost (window-based)/minimal (synchronous many-to-many)	Parallelism
Certification effort	Low	High	Moderate

not incur extra costs in online applications. Integrating deep learning models with model-based SOC estimation approaches for hybrid models has been implemented in research as well, where the overall scheme could have diverse layouts. Although the estimation of the neural networks is often used as the measurement, the developers have the liberty to choose different models, such as equivalent circuit models or simple coulomb counting models, for the prior estimates, namely the prediction. It was argued that both the accuracy and the robustness are enhanced by such hybrid SOC estimation models [111].

3.4. Appeal for a standardized evaluation protocol

It is obvious that the current SOC estimation works are based on a variety of different experimental setups, including utilized datasets, ways of data splitting, preprocessing procedures, and evaluation metrics, which makes the objective comparison between different studies difficult. In order to promote a standardized protocol for experimental setups, we appeal for the following proposals:

1. Use fixed dataset combination for model development. The proposed models should be evaluated on at least two different public datasets. Considering the aforementioned problem of data synthesis in the UW-Madison and McMaster datasets, the TU Berlin dataset and the CALCE dataset should be preferred.
2. Unify the procedure for data preprocessing and splitting. Use a separate validation set for hyperparameter fine-tuning and only report the models' performance on the unseen test set.
3. Include all common evaluation metrics: MAE, RMSE, and R^2. These evaluation metrics provide insights into the models' performance in different aspects and are universally used in regression tasks.
4. Test the model under all temperatures. Although 25 °C or the room temperature might be the most common case, different ambient conditions could lead to different performances of the model. Testing the developed model under all temperatures can not only provide an objective evaluation of its generalization ability but also reveal possible limitations.

This might only be a tiny step forward towards a universally acknowledged evaluation protocol in the field of SOC estimation. But in any case, we believe the attempt is worthwhile, as the field of SOC estimation can only march forward with a clear goal, which would be provided by a standardized evaluation protocol.

3.5. Decision framework for architecture selection

Table 4 is a lean summary of the trade-offs of different basic neural network architectures for SOC estimation, where FNNs, RNNs/LSTM/GRU, and CNNs/TCNs are compared with each other. For temporal modeling abilities, RNNs are particularly outstanding for long-term dependencies because of the information transfer through time via the hidden states. CNNs are suitable for moderate history via dilation or stacking the convolutional layers, while FNNs should only be prioritized for short-window mapping. However, FNNs have the lowest latency for real-time computation because of the simple forward pass operation, followed by CNNs with the more complicated convolutional operation, heavily dependent on the hardware parallel-computation efficiency. As for RNNs, two different ways of implementation should be discussed. The conventional window-based sequential style of implementation, where a window of historical data is fed into the network at each time step, induces high latency in real-time computation, as the operation must be conducted sequentially. On the other hand, the synchronous many-to-many style of implementation [112], where only the current input is fed into the network at each time step, with historical information transferred by the stored intermediate hidden states (stateful RNNs), induces low latency in real time. As to the comparison of computational cost, FNNs only have basic matrix multiplication and summation, causing low floating point operations (FLOPs). For RNNs, particularly LSTM and GRU, the computational cost is much higher if implemented in the window-based sequential way, as the mapping of the hidden state and the gating mechanisms has brought an extra burden on top of FNNs. However, if implemented in the synchronous many-to-many style, the computational cost becomes minimal for temporal modeling, as no history windows are considered. For CNNs, although a considerable number of convolutional operations have to be done, but they can be highly parallel. As for parameter count, often FNNs have the largest number of weights and biases, as a wide input window is needed for the flattened temporal features over multiple time steps. With the help of shared kernels and dilation, CNNs are able to reduce the parameter count to a moderate level. RNNs often have the lowest parameter count compared to the other two architectures, especially in the case of long-term dependency modeling, as the input at each time step is only one vector due to the recursive nature. Overall, the bottlenecks for onboard applications in embedded systems for the networks are: memory cost for FNNs due to the huge amount of parameters, latency and computational cost for window-based RNNs, parallelism in computation for CNNs, and there is minimal bottleneck for synchronous many-to-many RNNs. Safety certification is another important factor for commercial use. FNNs should be the ones with the lowest certification effort because of their simple architecture and predictable behaviors. CNNs should have a moderate level of certification effort because of the relatively clear path of convolutional operation. RNNs with LSTM and GRU are the hardest for safety certification because of the complicated temporal paths of hidden states and multiple gating mechanisms. Based on the analysis, Procedure 1 is a concise decision tree for model architecture selection for deep learning-based SOC estimation.

4. Emerging perspectives

Deep learning-based SOC estimation methods have advanced tremendously in recent years, showing great potential in improving

Procedure 1: Procedure for model architecture selection for SOC estimation.

Step 1: What history length needs to be modeled?

a) Short-term dependencies: go to **Step 2**.
b) Long-term dependencies: go to **Step 3**.

Step 2: For short-term mapping, which factor is highest priority?

a) Lowest latency & easiest certification: **FNNs**.
b) Memory constraints: **RNNs**.
c) Strong parallel hardware or universal compromise: **CNNs**.

Step 3: For long-term modeling, is the computation budget very limited?

a) Yes: **synchronous many-to-many RNNs**.
b) No: go to **Step 4**.

Step 4: Is the memory budget very limited?

a) Yes: **window-based RNNs**.
b) No: go to **Step 5**.

Step 5: What other priority exists?

a) Strong hardware parallelism or universal compromise: **CNNs**.
b) Strict certification & ultra low latency : **FNNs**.

estimation accuracy and adaptability. At the same time, the rapid development of battery technologies and the versatility of application scenarios pose brand-new challenges. To accommodate this background, researchers have delved into the emerging perspectives with state-of-the-art deep learning frameworks and paradigms to further improve deep learning-based SOC estimation comprehensively in different aspects. In this section, we summarize the emerging perspectives in the research field of deep learning-based SOC estimation of lithium-ion batteries, including physics-informed neural networks (PINNs), multi-task learning (MTL), few-shot learning, and continual learning. Despite the fact that some other special techniques [113] can seemingly be add-ons for deep-learning SOC estimation, such as automated machine learning [114–116], these four pioneering areas have been selected as the emerging perspectives in this review because of the following critical factors:

1. Each technique targets a core SOC-estimation bottleneck:

    (a) First, traditional data-driven models rely completely on high-quality datasets and black-box modeling without the possibility for the integration of validated prior knowledge. PINNs revolutionarily introduce physics laws as extra constraints that guide the learning of the neural networks. By leveraging the existing battery domain knowledge, PINNs reduce the requirements on the amount of high-quality training data and result in stronger generalization abilities of the model, which serves as one big step in opening the black box as well.
    (b) Second, SOC is highly correlated with other states like state of health (SOH) and state of energy (SOE) in real-life applications, while single-task SOC estimation models are not able to learn from these interactions. For that purpose, MTL models are dedicated to information sharing between correlated tasks in order to improve learning efficiency and generalization abilities, which increases not only the performance of SOC estimation, but also the efficiency of each data sample in the training.
    (c) Third, the acquisition of high-quality data has always been a major challenge for data-driven solutions, which becomes particularly prominent with the rapid iteration of commercial lithium-ion batteries. Appropriately labeled cycling data might be very scarce for some new battery types or under extreme cycling conditions, where neural networks without specific strategies can hardly achieve good performance. To mitigate the plight caused by limited data, few-shot learning techniques are specifically designed to help deep learning models generalize on small datasets, thereby significantly accelerating the development of new SOC estimation models and reducing the efforts and costs in data collection.
    (d) Fourth, again, with the accelerated iteration of commercial lithium-ion batteries, hybrid energy storage systems consisting of different types of batteries are gaining increasing potential benefits. On the other hand, it would be time-consuming if the SOC estimation model needs to be retrained from scratch whenever a new type of cell is integrated into an existing energy storage system in reality. Furthermore, simple incremental training without specific measures would lead to the catastrophic forgetting of the model's old knowledge on the existing cells [117]. With continual learning techniques, the on-board SOC estimation models can not only already be optimized for the simultaneous accurate estimation of existing hybrid battery systems before deployment, but also adaptively be updated for the new cells while maintaining previously learned knowledge.

2. Each technique shows a marked uptick in recent publications. We conducted a literature search to validate the number of related publications per year indexed by Google Scholar in two different cases: the original techniques as keywords, and the techniques applied in the battery field as keywords.

    (a) In the first case, the four keywords, namely "Physics-informed neural networks", "Multi-task learning", "Few-shot", "Continual learning", have been applied for the literature search, which is aimed at validating the overall development and growth of popularity of each technique per se in different research fields. As shown in Fig. 7(a), all four techniques have gained growing attention from 2018 to 2024. In the year 2018, the number of related publications was 368, 5060, 1040, 1660, respectively, for each technique, which went up to 11 300, 24 500, 56 500, 13 200 by the end of 2024. The number of indexed publications has increased in the past 7 years by approximately 30 times, 5 times, 54 times, and 8 times, respectively, for PINNs, MTL, few-shot learning, and continual learning. The degree of increase is particularly drastic for few-shot learning, demonstrating the current research trend in application scenarios where the deep learning models need to generalize with limited data, which can be attributed to the conflict between the growing demand for an enormous amount of labeled high-quality data for modern deep learning models and the high cost in time and money of acquiring it.
    (b) In the second case, the four keywords, namely "Physics-informed neural networks" AND "SOC" AND "Battery", "Multi-task learning" AND "SOC" AND "Battery", "Few-shot" AND "SOC" AND "Battery", have been applied for the literature search, which is aimed at checking the growth of attention they receive specifically in the

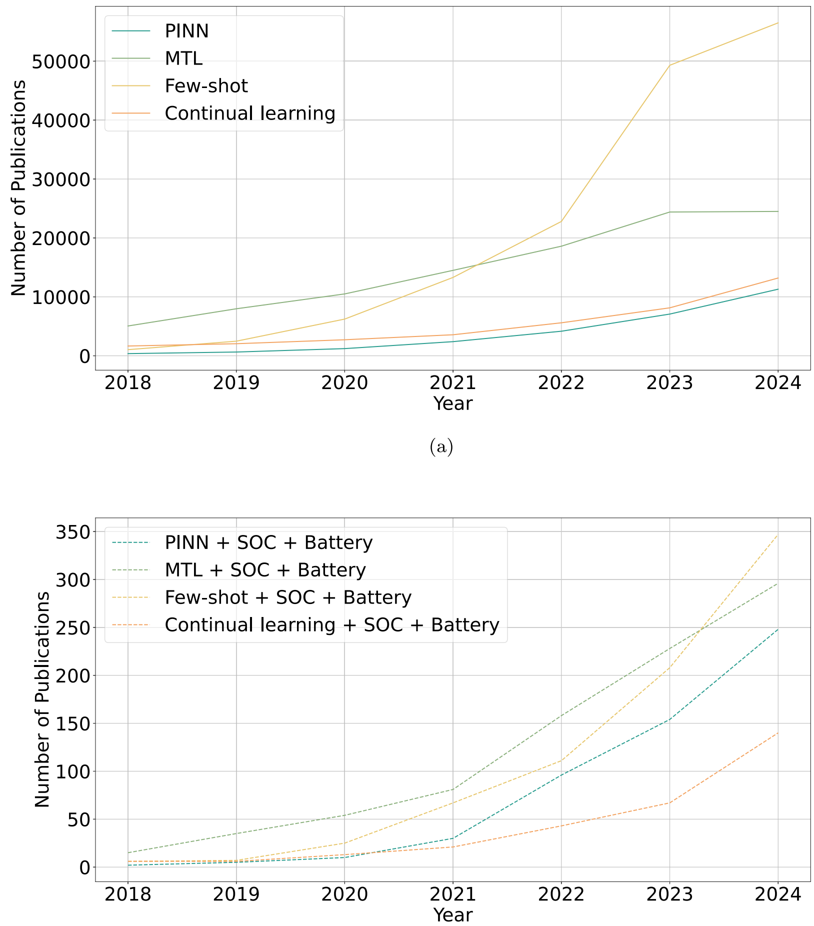

(a)

(b)

Fig. 7. Number of related publications per year indexed by Google Scholar. (a) The original techniques as keywords. (b) The techniques applied in the battery field as keywords.

field of battery state estimation. It is worth mentioning that each indexed work does not necessarily focus on SOC estimation itself, but certainly has covered related discussions. As shown in Fig. 7(b), significant growth of received attention in the field of battery state estimation can be observed for all techniques. In the year 2018, the number of related publications was 2, 15, 6, 6, respectively, for each technique, which went up to 248, 296, 347, and 140 by the end of 2024, indicating an increase by approximately 124 times, 20 times, 58 times, and 23 times, respectively. This trend clearly suggests the selected four techniques have been gaining increasing attention in the research field of battery state estimation, hence the emerging perspectives.

4.1. Physics-informed neural networks

Ordinary deep learning models are purely data-driven and thus fully rely on the available training data. Such black-box implementation brings uncertainty into the estimation process so that the models can make estimations that do not conform to the actual physical laws. In addition, the performance of purely data-driven models is completely dependent on the quantity and quality of the available data, posing great challenges to the collection and preprocessing of high-quality data. To solve the aforementioned problems for purely data-driven models, PINNs [118] arise in response. By integrating the knowledge of physical laws into the learning process, PINNs are trained under the guidance of prior information and are less dependent on the data at hand, resulting in a better learning outcome, stronger generalization ability, and fewer requirements on the amount of training data. As physical laws often appear in the form of partial differential equations (PDEs), PINNs are able to leverage the automatic differentiation in the deep learning frameworks to compute the required derivatives conveniently.

In the context of SOC estimation, known electrochemical models, such as the single-particle model or the Doyle-Fuller-Newman (DFN) model, can be introduced in PINNs. By embedding the physical constraints as an extra term of losses, PINNs for SOC estimation could benefit from the guidance of the known physical laws. Fig. 8 is an example framework of PINNs for SOC estimation. By leveraging both the physics-based information and the measurement information, the model is able to learn and benefit from both. In Ref. [119], the authors proposed a PINN for joint SOC and SOH estimation of lithium-ion batteries. The proposed PINN takes the radial coordinate and time as input and predicts the lithium-ion solid-phase concentration. Subsequently, the single-particle model of lithium-ion batteries is utilized as the electrochemical model that governs the physical process, where two porous spherical particles are used to represent the two electrodes as simplification as the embedded physical information. The loss term originated from the physical constraints consists of three parts, namely Fick's law of diffusion, Neumann boundary conditions, and the initial condition of the solid-phase concentration of lithium ions. Together with the data-driven loss term, the network is trained based on the backpropagation of the total loss. Experimental results showed that the proposed PINN was able to deliver satisfying SOC estimation results with limited training data for unseen scenarios, where the RMSE lies

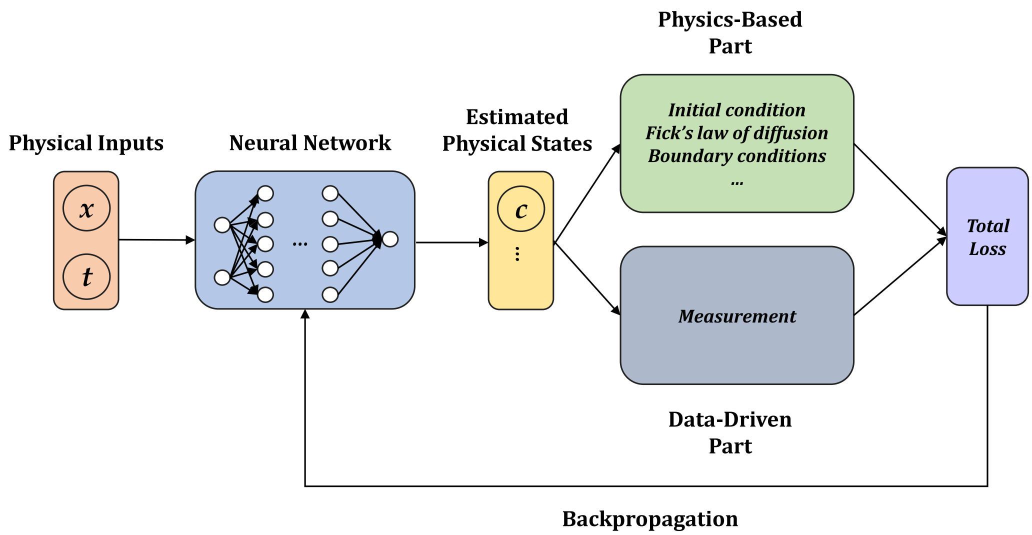

Fig. 8. An example framework of physics-informed neural networks for SOC estimation.

in the range from 0.014% to 0.20%. The loss curves during training showcased a decreasing trend until convergence, directly indicating that the developed PINN has gained the ability to simulate the internal electrochemical processes of the batteries by learning from the physics laws, thus increasing the interpretability of the original black-box neural network. In Ref. [120], the authors established an extended single-particle model and utilized a PINN to solve it for the purpose of SOC estimation. The PINN takes the positional information, time, cycling current, and initial lithium-ion concentration on the particle surface as input, and solves the lithium-ion concentration distribution on the particle surface and in the electrolyte. The current SOC can be calculated based on the mean concentration of the lithium ions of the solid particles of the respective electrode. The proposed PINN was able to solve the electrochemical model tremendously faster than the traditional numerical method. Results show that PINNs can model the lithium-ion concentration on the surface of the anode accurately compared with COMSOL solutions, indicating that PINNs have acquired a deep understanding of the internal electrochemical dynamics, granting the data-driven vanilla neural networks enhanced interpretability.

Besides the classical implementation of PINNs where PDEs are embedded and solved, some other works have made their attempts to integrate physical information into deep learning models for SOC estimation in different fashions as well, where the models can be called PINN in a broad sense. In Ref. [121], the authors proposed a PINN for SOC estimation of lithium-ion batteries, where the coulomb counting model is integrated into the loss calculation instead of using complicated electrochemical models. Results showed that the developed PINN outperforms the traditional neural network FNN and the adaptive Kalman filter (AKF) on the test set. The developed PINN achieved the MAEs of 2.0260%, 1.4987%, 1.7780%, and 2.3287%, respectively, under −10 °C, 0 °C, 10 °C, and 25 °C on the test set, outperforming the corresponding MAEs of 2.4967%, 2.1460%, 1.7028%, 2.3688% for the FNN and the corresponding MAEs of 3.2824%, 3.1595%, 2.5961%, 1.9393% for the AKF in most cases. In Ref. [122], the authors incorporated the prior information of an equivalent circuit model into the PINN framework. In Ref. [123], the authors proposed a physics-informed RNN for SOC estimation of lithium-ion batteries by introducing fractional-order gradients into the backpropagation process. In Ref. [124], the physical domain knowledge was incorporated into the deep learning model in two ways. First, equivalent circuit models were used to decouple the voltage and current readings into the OCV and overvoltages, which were subsequently used as the input of the deep learning model. Second, the Kalman filter was used to fuse the SOC estimation from the deep learning model and the coulomb counting model. Test results showed that the proposed approach reduced the SOC estimation error significantly with little increased computational costs. At 25 °C, the LSTM model with integrated physical domain knowledge was able to achieve the MAEs of 1.76%, 1.44%, and 1.32% on the test set, respectively, for implementing only the first way of integration, implementing only the second way of integration, and implementing both. In comparison, the LSTM model without physical domain knowledge integration could only achieve an MAE of 1.91%. Despite the fact that these models do not correspond strictly to the original PINN framework, they all attempted to introduce physical information and prior domain knowledge into purely data-driven deep learning models, and the results appeared promising, which might have shed light on how we can open up the black-box deep learning models.

In real-life applications, PINNs can effectively mitigate unreasonable estimations in radical conditions caused by pure data-driven models by sticking to the validated physics law. In addition, the integration of domain knowledge decreases the amount of required data. However, PINNs might lead to more complicated network training and higher computational consumption due to the automatic gradient calculation, making them harder to implement in embedded systems. Furthermore, domain experts are needed for the selection of integrated physics laws for PINNs. Therefore, a possibility for the practical utilization of PINNs might require advanced pruning or simplification of the offline-trained PINNs. Hardware specially designed for accelerated PDE derivation and inference might be a must in this case as well.

4.2. Multi-task learning

Conventional deep learning models are trained for specific tasks individually, which in many cases cuts off the opportunity for the models to benefit from the information of related tasks in order to further enhance the performance [125]. Multi-task learning is a deep learning paradigm where multiple related tasks are learned simultaneously. By exploiting the shared information and the complementary representations between different tasks, the learning efficiency and generalization ability are improved for MTL models [125,126]. Generally speaking, MTL approaches can be categorized into hard parameter sharing and soft parameter sharing [125], as shown in Fig. 9. In hard parameter sharing, different tasks exploit the same shared bottom layers while having some task-specific layers for each output. By using the same backbone for feature extraction, hard parameter sharing increases the generalization ability of the model by forcing it to learn the more general features and thus reduces the risk of overfitting. In addition, using shared layers decreases the memory and computational costs

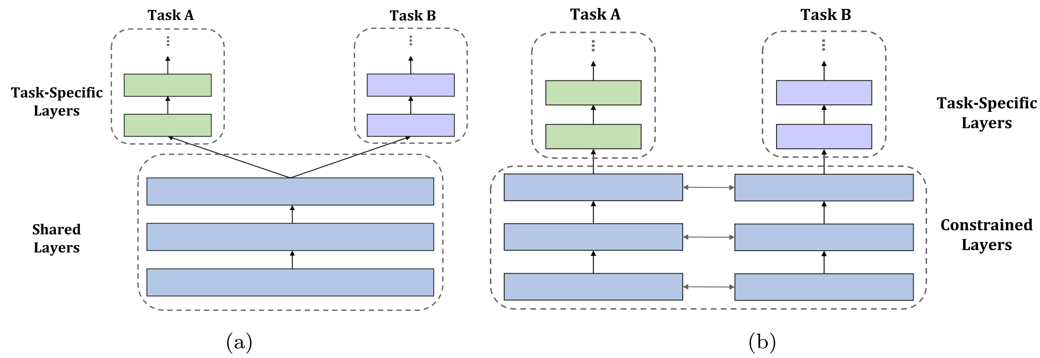

Fig. 9. MTL classification. (a) Hard parameter sharing. (b) Soft parameter sharing.

of the model. However, such implementation could lead to a lack of flexibility in feature extraction for different tasks, imposing the prerequisite that the target tasks must be closely related. On the other hand, soft parameter sharing utilizes regularization techniques to impose constraints on the bottom layers, so that they would learn the shared information. Such implementation allows the models to have their own parameters but still learn the tasks collectively in a free fashion. Modern MTL techniques are mostly based on soft parameter sharing, such as cross-stitch networks [127], sluice networks [128], and multi-gate mixture-of-experts (MMoE) [129].

The internal states of lithium-ion batteries, such as SOC, SOH, and SOE, are closely related to each other. In practice, other key states should also be taken into consideration for an accurate SOC estimation. By utilizing MTL approaches to capture the shared information between different states, the deep learning models can benefit from feature sharing and information complementation and gain enhanced estimation accuracy and robustness. In Ref. [130], the authors combined hard parameter sharing with MMoE for the joint estimation of SOC and SOE of lithium-ion batteries. Two LSTM layers are used as the shared bottom to extract the preliminary features from the time series data. The extracted features are then processed by an MMoE module, where one shared expert and two task-specific experts are regulated by two gates. The loss weighting method, dynamic weight average (DWA) [131], was experimented with in the work as well. Test results on the UW-Madison dataset and the McMaster LG dataset showed that the proposed MTL model was able to outperform single-task models and other commonly seen MTL models with better estimation accuracy and generalization ability, where an MAE of 0.5943% was achieved by the proposed MTL model on the UW-Madison dataset, outperforming the MAE of 0.6456% of the traditional single-task model. In Ref. [132], the authors proposed a transferred MTL model for online state monitoring of SOC, SOE, and temperature. The proposed MTL model is based on hard parameter sharing, which takes current, voltage, temperature, and differential temperature as input. 1D convolutional layers are used as the bottom layers to learn the shared representation, which is then fed into three sets of fully connected layers for the regression of each output. Experiments conducted with diverse cycling and aging conditions showcased that the proposed transferred MTL model improved the estimation accuracy significantly and was able to deliver an accurate temperature prediction with a horizon of five steps. In our previous work [112], we proposed an MTL model for joint SOC and SOH estimation of lithium-ion batteries which combines cross-stitch networks and hard parameter sharing. The network takes the voltage, current, and temperature measurements as input, and produces the online estimates of SOC and SOH. A shared LSTM is utilized to capture the fundamental underlying patterns, which are then fed into both the SOC tower and SOH tower for further feature extraction. Between the two task-specific towers, multiple cross-stitch units are used to linearly combine the learned feature vectors, enabling the free information flow between the two tasks. Different weighting methods were experimented with, including empirical weighting, uncertainty weighting, and DWA, where the weighting method of empirical weighting appeared to perform the best. The learning process of the cross-stitch units showed that the determination of SOC benefits from the information of SOH, which was also proved by the experimental results where the SOC estimation of the model tested on dynamic profiles with an MAE of 0.786% outperformed the single-task model with an MAE of 1.690% significantly. In Ref. [133], the authors introduced an MTL framework for joint SOC and SOE estimation of lithium-ion battery packs. The proposed framework is based on hard parameter sharing, where a GRU layer and an attention layer are used as the shared bottom taking the maximum voltage, minimum voltage, and pack voltage as input. Comprehensive experimental results on real operational data of electric vehicles showcased the high accuracy of the proposed framework for SOC and SOE estimation with MAEs below 1.4% and R^2 over 99.6%.

The adoption of MTL models not only increases the performance of the estimation of diverse key internal states of the battery systems but also mitigates the high memory and computational cost of deep learning models. As seen in the research field of SOC estimation recently, an increasing number of works are focusing on deep learning-based joint state estimation of lithium-ion batteries using MTL, which, in fact, is perfectly compliant with the trend of having multi-functional intelligent BMSs on board. Therefore, we believe the development of deep learning models with MTL paradigms is going to be a hotspot in the research field.

As for practical applications, the multi-tasking nature of MTL models saves memory and computational costs significantly in embedded systems while increasing the accuracy of different estimation tasks. However, it also poses more challenges in the network design and offline training. The architecture of MTL models must be carefully adjusted for each task, as well as the extra hyperparameters, such as the weights of losses. In embedded environments, the deployed MTL models need to be completely tuned again as a whole in case of task updates or switching. Practitioners are recommended to first develop their MTL models offline with small dataset samples for the evaluation of different architectures and hyperparameter designs, and then upscale their model to practical scenarios. More flexible ways of information sharing between tasks might be beneficial in order to minimize the additional cost for network fine-tuning in case of task updating.

4.3. Few-shot learning

The successful development of deep learning models is greatly dependent on the quantity of high-quality datasets. In practice, however, challenges often occur as the acquisition and annotation of such large-scale and high-quality data are very time-consuming and not always possible due to a variety of limitations. In the context of SOC estimation of lithium-ion batteries, dynamic cycling data of different battery cells that cover diverse usage patterns and operation conditions can be hard for developers and researchers to obtain. As a result, accessible data on certain battery types may be scarce or imbalanced, leading to insufficiently trained models with little generalization ability. Few-shot learning is a branch of machine learning that aims at training models on limited data samples for sufficient generalization abilities [134]. Existing few-shot learning approaches can be categorized into three types based on the aspects enhanced by the introduced prior knowledge: data-based, model-based, and algorithm-based [135]. In data-based few-shot learning, prior knowledge is utilized to augment and enlarge the dataset, while model-based few-shot learning approaches aim at restraining the size of the hypothesis space and algorithm-based few-shot learning approaches aim at finding the best hypothesis in the given space based on prior knowledge [135].

Among all the few-shot learning methods, meta-learning is one of the most commonly used approaches, which aims at obtaining a model that can rapidly adapt to new tasks with minimal fine-tuning by designing a training paradigm over multiple tasks that urges the model to "learn to learn". In recent years, a variety of meta-learning methods have been proposed, such as the optimization-based approach model-agnostic meta-learning (MAML) [136], and metrics-based methods like Siamese neural networks [137], matching networks [138], and prototypical networks [139]. In order to tackle the aforementioned high demands on cycling data for the development of SOC estimation models, researchers have applied meta-learning as well. In Ref. [140], the authors proposed a meta-learning method that utilizes MAML for SOC estimation of lithium-ion batteries with little target training data. The updating of the meta-parameters is performed by an outer loop containing an inner loop. In the inner loop for each task, gradient updates of a few steps are performed based on the training data of the respective task. Losses are calculated based on the updated model on each task's test set, which are then used as the meta-loss to update the meta-parameters in the outer loop. In this way, the model is forced to learn the best initialization that can rapidly adapt to new tasks. Four public datasets, namely the UW-Madison dataset, the two McMaster datasets, and the CALCE NMC dataset were used for the experiments of the comparison between the proposed meta-learning approach with transfer learning, which showed that meta-learning reduces the amount of required training data of the target battery significantly by utilizing the data from other types of batteries. In addition, the learning process of the model can also be tremendously accelerated using meta-learning for pre-training, resulting in a faster development of the SOC estimation models. Experimental results showed that the model pretrained with meta-learning was able to achieve an MAE of 1.0075% on the US06 cycle after fine-tuning with 96 data points and 9 gradient steps, outperforming the three models pretrained with transfer learning (15.1327%, 18.7724%, 19.4432% MAE), the FNN model (20.0868% MAE), the LSTM model (6.4132% MAE), and the GRU model (4.0124% MAE).

Although there have not been many pieces of research focusing on the few-shot learning aspect of SOC estimation of lithium-ion batteries, we believe it is a research topic that can be of great potential to real-life applications, as there is an increasing demand for battery management systems on adapting to new types of lithium-ion batteries and operating conditions relying on limited data, possibly due to privacy issues. In addition, the adoption of few-shot learning techniques could accelerate the prototyping procedure and improve the generalization abilities of the estimation models.

When it comes to real-life application scenarios, SOC estimation models with few-shot learning techniques have great commercial value as they are perfectly suitable for cases like when vehicle manufacturers have to rapidly prototype their battery systems with shortened algorithm development cycles by lowering the need for an enormous amount of labeled data under a new environment. However, few-shot learning approaches might require diverse task datasets with different types of batteries and cycling conditions to start with, and their robustness needs to be carefully validated, especially for safety-critical applications. Therefore, the developers are recommended to carefully think through whether the datasets they have at hand fit the few-shot learning algorithms' requirements before implementation. Meanwhile, the developers should consider integrating data augmentation methods, such as generative models, to expand the pool of task datasets.

4.4. Continual learning

Battery technology has made tremendous progress in recent years, which, on the other hand, accelerates the iteration of commercial lithium-ion battery cells significantly. Against this background, hybrid battery systems that incorporate diverse types of batteries have stepped up [141]. In addition, the adoption of hybrid lithium-ion battery packs can leverage the advantages of diverse lithium-ion batteries [142] and achieve a trade-off between high-energy and high-power lithium-ion cells [143]. Although there have been precedent research works dedicated to model-based SOC estimation in hybrid battery packs [144], conventional deep learning for SOC estimation of different types of batteries is inherently challenging because of the so-called catastrophic forgetting, where deep learning models forget about the previously learned knowledge on old tasks when trained with new tasks [145]. To deal with this challenge, the research branch of continual learning has come into existence [146], which aims at preserving previously learned knowledge on old tasks while incrementally learning new tasks and letting the model benefit from both forward (old to new) and backward (new to old) knowledge transfer [147]. In general, continual learning methods can be categorized into replay-based methods, regularization-based methods, and parameter isolation-based methods [148]. Continual learning techniques have been applied in some works on battery degradation prediction [149] and SOH estimation [150], but all in the purpose of dynamically updating the model to adapt to drifting data distribution of the test batteries. In Ref. [117], we proposed a continual learning framework for online SOC estimation across diverse lithium-ion batteries, which appeared to be the first to apply continual learning techniques to SOC estimation of different types of lithium-ion batteries. The parameter isolation-based continual learning framework, progressive neural networks (PNNs), was utilized to learn new tasks with the previously learned knowledge intact by using a dynamically augmented network architecture. In PNNs, each column is instantiated for one task, where lateral connections between different columns are utilized to enable the information flow between different tasks. While trained on new tasks, the parameters of the previous columns are frozen, so that the model's performance on old tasks will not be affected, which makes the PNN framework immune to catastrophic forgetting by design. TCNs are used to extract temporal features efficiently in the network. Experimental results on three public datasets, namely the UW-Madison dataset, the McMaster Samsung dataset, and the TU Berlin dataset showed that the proposed continual learning framework was not only able to deliver state-of-the-art SOC estimation accuracy for each task after incrementally trained on different tasks, but also reduced the model complexity through the positive knowledge transfer enabled by the lateral connections. Results showed that after incrementally learned all three tasks, the average accuracy of the proposed PNN model was as high as 99.001%, significantly outperforming the average accuracy of 84.703% for the vanilla incremental learning model without continual learning strategies, and even the average accuracy of 98.644% for the reference single-task models.

Similar to few-shot learning, continual learning for SOC estimation of diverse lithium-ion batteries is also an emerging perspective in the research field that can potentially bring great practicality into real-life applications. We think this is a research topic that is going to come to light with the increasing usage of hybrid battery systems.

In practice, SOC estimation models with continual learning techniques would save practitioners a great amount of costs in onboard applications as well, as the comprehensive iteration of the massive amount of historical data can be mitigated in case of battery update, where the models only need to be fine-tuned for the new task. However, existing continual learning methods might bring extra memory and computational burden to the onboard systems. For example, PNNs would have increasingly more columns with more tasks, leading to a high memory cost in the long term, which is the same for replay-based methods, where historical samples need to be stored. For regularization-based methods, the online updating of the networks would require higher computational consumption. Therefore, the developers should consider carrying out the training offline on the cloud and integrating pruning techniques to keep the continual learning models lightweight.

5. Conclusion

An accurate SOC estimation of lithium-ion batteries is the cornerstone of a safe and optimized operation. With the drastic advances in the research field of deep learning in recent years, SOC estimation based on it has made significant progress as well. This review article carries out a structured review on the existing deep learning-based approaches for SOC estimation and the current emerging perspectives in the research field. A comprehensive introduction to the technical background is provided, including a detailed taxonomy of SOC estimation approaches and popularly used public datasets for the development of data-driven SOC estimation models. We present a systematic walk-through of the existing deep learning-based SOC estimation approaches for lithium-ion batteries together with the frequently applied optimization strategies in the research field. In our survey of 24 deep learning-based SOC estimators, FNNs achieve MAEs in the range of 0.093%–1.35%, RNNs achieve MAEs in the range of 0.091%–2.02%, and CNNs achieve MAEs in the range of 0.363%–2.56%, resulting in a median MAE of 0.73% for FNNs, a median MAE of 0.814% for RNNs, and a median MAE of 0.641% for CNNs. However, it is worth mentioning that the performance of the proposed models of each work cannot be directly compared with each other quantitatively, as the utilized cell types and experimental setups differ from work to work. Therefore, we appeal for a standardized evaluation protocol for the field of SOC estimation to enable objective comparison between models. As highlight, the current trends and emerging perspectives of deep learning-based SOC estimation are pointed out and discussed in detail, which can be summarized as follows:

1. By incorporating physical constraints into the data-driven models, PINNs can benefit from the guidance of physical prior knowledge and open up the black-box deep learning models for state estimation of lithium-ion batteries.
2. The adoption of MTL models not only improves the performance of estimation but also mitigates the high memory and computational cost, which is perfectly compliant with the trend of having multi-functional intelligent BMSs on board.
3. Few-shot learning techniques, especially meta-learning, appear to be a versatile way of pre-training deep learning models for SOC estimation, as they reduce the required amount of training data and accelerate the prototyping procedure.
4. With the rapid iteration of commercial lithium-ion battery cells, the increasingly profitable usage of hybrid battery systems could benefit from continual learning-based SOC estimation models tremendously, where one deep learning model can be used for diverse lithium-ion batteries with optimized estimation accuracy and model complexity.

We believe this work not only provides researchers and practitioners new to this topic with a clear and detailed manual to start with, but also points out the emerging perspectives for further cutting-edge studies towards a smarter battery management system.

Abbreviations

The following abbreviations are used in this manuscript:

AKF	Adaptive Kalman Filter
Adaptive UKF	AUKF
Bi-GRU	Bidirectional GRU
Bi-LSTM	Bidirectional LSTM
BJDST	Beijing Dynamic Stress Test
BMS	Battery Management System
BPNN	Backpropagation Neural Network
BSA	Backtracking Search Algorithm
CALCE	Center for Advanced Life Cycle Engineering
CC-CV	Constant Current-Constant Voltage
CNN	Convolutional Neural Network
CVA	Canonical Variate Analysis
CWRNN	Clockwork Recurrent Neural Network
DAE	Denoising Autoencoder
DFN	Doyle-Fuller-Newman
DNN	Deep Neural Network
DST	Dynamic Stress Test
DWA	Dynamic Weight Average
EI-LSTM-CO	LSTM with Extended Input and Constrained Output
EIS	Electrochemical Impedance Spectroscopy
EKF	Extended Kalman Filter
FA	Firefly Algorithm
FC	Fully Connected
FLOPs	Floating Point Operations
FNN	Feedforward Neural Network
FUDS	Federal Urban Driving Schedule
GA	Genetic Algorithm
GRU	Gated Recurrent Unit
GRU-ATL	GRU with Activation Function Layers
HPO	Hyperparameter Optimization
HPPC	Hybrid Pulse Power Characterization
HWFET	Highway Fuel Economy Test
LA92	California Unified Cycle
LFP	Lithium Iron Phosphate
LSTM	Long Short-Term Memory
MAE	Mean Absolute Error
MLP	Multilayer Perceptron
MMoE	Multi-Gate Mixture-of-Experts
MTL	Multi-Task Learning
NAG	Nesterov Accelerated Gradient
NCA	Lithium Nickel Cobalt Aluminum
NEDC	New European Driving Cycle
NMC	Lithium Nickel Manganese Cobalt
OCV	Open Circuit Voltage
PDE	Partial Differential Equation
PDMHC	Port Drayage Metro Highway Cycle California
PINN	Physics-Informed Neural Network
PNN	Progressive Neural Network
ReLU	Rectified Linear Unit
SG-BiLSTM	Savitzky-Golay filter-based bidirectional LSTM
SOC	State of Charge
SOE	State of Energy
SOH	State of Health
SVM	Support Vector Machine
TCN	Temporal Convolutional Network
TPE	Tree Parzen Estimator
UDDS	Urban Dynamometer Driving Schedule
UKF	Unscented Kalman Filter
UW-Madison	University of Wisconsin-Madison
US06	US06 Supplemental Federal Test Procedure

CRediT authorship contribution statement

Jiaqi Yao: Writing – review & editing, Writing – original draft, Visualization, Validation, Software, Resources, Methodology, Investigation, Formal analysis, Data curation, Conceptualization. **Julia Kowal:** Writing – review & editing, Supervision.

Declaration of competing interest

The authors declare that they have no known competing financial interests or personal relationships that could have appeared to influence the work reported in this paper.

Acknowledgment

We thank the Open Access Publication Fund of TU Berlin for the support.

Data availability

No data was used for the research described in the article.

References

[1] Diouf B, Pode R. Potential of Lithium-Ion batteries in renewable energy. Renew Energy 2015;76:375–80. http://dx.doi.org/10.1016/j.renene.2014.11.058.
[2] Horiba T, Maeshima T, Matsumura T, Koseki M, Arai J, Muranaka Y. Applications of high power density Lithium Ion batteries. J Power Sources 2005;146(1–2):107–10. http://dx.doi.org/10.1016/j.jpowsour.2005.03.205.
[3] He W, Guo W, Wu H, Lin L, Liu Q, Han X, Xie Q, Liu P, Zheng H, Wang L, Yu X, Peng D-L. Challenges and recent advances in high capacity li-rich cathode materials for high energy density Lithium-Ion batteries. Adv Mater 2021;33(50):2005937. http://dx.doi.org/10.1002/adma.202005937.
[4] Kim GY, Park SR, Yu JS. Design and characteristics of low-resistance lithium-ion battery pack and its fast charging method for smart phones. Int J Energy Res 2021;45(12):17631–46. http://dx.doi.org/10.1002/er.7079.
[5] Liang Y, Zhao C-Z, Yuan H, Chen Y, Zhang W, Huang J-Q, Yu D, Liu Y, Titirici M-M, Chueh Y-L, Yu H, Zhang Q. A review of rechargeable batteries for portable electronic devices. InfoMat 2019;1(1):6–32. http://dx.doi.org/10.1002/inf2.12000.
[6] S. Rangarajan S, Sunddararaj SP, Sudhakar A, Shiva CK, Subramaniam U, Collins ER, Senjyu T. Lithium-Ion batteries—The crux of electric vehicles with opportunities and challenges. Clean Technol 2022;4(4):908–30. http://dx.doi.org/10.3390/cleantechnol4040056.
[7] Lai X, Chen Q, Tang X, Zhou Y, Gao F, Guo Y, Bhagat R, Zheng Y. Critical review of life cycle assessment of Lithium-Ion batteries for electric vehicles: A lifespan perspective. ETransportation 2022;12:100169. http://dx.doi.org/10.1016/j.etran.2022.100169.
[8] Camargos PH, Dos Santos PHJ, Dos Santos IR, Ribeiro GS, Caetano RE. Perspectives on Li-ion battery categories for electric vehicle applications: A review of state of the art. Int J Energy Res 2022;46(13):19258–68. http://dx.doi.org/10.1002/er.7993.
[9] Steckel T, Kendall A, Ambrose H. Applying levelized cost of storage methodology to utility-scale second-life Lithium-Ion battery energy storage systems. Appl Energy 2021;300:117309. http://dx.doi.org/10.1016/j.apenergy.2021.117309.
[10] Bai H, Song Z. Lithium-Ion battery, sodium-ion battery, or redox-flow battery: A comprehensive comparison in renewable energy systems. J Power Sources 2023;580:233426. http://dx.doi.org/10.1016/j.jpowsour.2023.233426.
[11] Choi D, Shamim N, Crawford A, Huang Q, Vartanian CK, Viswanathan VV, Paiss MD, Alam MJE, Reed DM, Sprenkle VL. Li-ion battery technology for grid application. J Power Sources 2021;511:230419. http://dx.doi.org/10.1016/j.jpowsour.2021.230419.
[12] Gabbar H, Othman A, Abdussami M. Review of Battery Management Systems (BMS) development and industrial standards. Technol 2021;9(2):28. http://dx.doi.org/10.3390/technologies9020028.
[13] Hossain Lipu M, Hannan M, Karim TF, Hussain A, Saad MHM, Ayob A, Miah MS, Indra Mahlia T. Intelligent algorithms and control strategies for battery management system in electric vehicles: Progress, challenges and future outlook. J Clean Prod 2021;292:126044. http://dx.doi.org/10.1016/j.jclepro.2021.126044.
[14] Xiong R, Cao J, Yu Q, He H, Sun F. Critical review on the battery state of charge estimation methods for electric vehicles. IEEE Access 2018;6:1832–43. http://dx.doi.org/10.1109/ACCESS.2017.2780258.
[15] Khan N, Ooi CA, Alturki A, Amir M, Shreasth, Alharbi T. A critical review of battery cell balancing techniques, optimal design, converter topologies, and performance evaluation for optimizing storage system in electric vehicles. Energy Rep 2024;11:4999–5032. http://dx.doi.org/10.1016/j.egyr.2024.04.041.
[16] Chavan S, Venkateswarlu B, Salman M, Liu J, Pawar P, Joo SW, Choi GS, Kim SC. Thermal management strategies for Lithium-Ion batteries in electric vehicles: Fundamentals, recent advances, thermal models, and cooling techniques. Int J Heat Mass Transfer 2024;232:125918. http://dx.doi.org/10.1016/j.ijheatmasstransfer.2024.125918.
[17] Yang F, Mao Q, Zhang J, Bao G, Cheng KWE, Lam K-H. Novel joint algorithm for state-of-charge estimation of rechargeable batteries based on the back propagation neural network combining ultrasonic inspection method. J Energy Storage 2024;99:113391. http://dx.doi.org/10.1016/j.est.2024.113391.
[18] E.P. S, N. S, T.K. S, S. AL, D. U. Validation of EKF based SoC estimation using vehicle dynamic modelling for range prediction. Electr Power Syst Res 2024;226:109905. http://dx.doi.org/10.1016/j.epsr.2023.109905.
[19] Demirci O, Taskin S, Schaltz E, Acar Demirci B. Review of battery state estimation methods for electric vehicles - Part I: SOC estimation. J Energy Storage 2024;87:111435. http://dx.doi.org/10.1016/j.est.2024.111435.
[20] Xing Y, He W, Pecht M, Tsui KL. State of charge estimation of Lithium-Ion batteries using the open-circuit voltage at various ambient temperatures. Appl Energy 2014;113:106–15. http://dx.doi.org/10.1016/j.apenergy.2013.07.008.
[21] Jin Y, Zhao W, Li Z, Liu B, Wang K. SOC estimation of Lithium-Ion battery considering the influence of discharge rate. Energy Rep 2021;7:1436–46. http://dx.doi.org/10.1016/j.egyr.2021.09.099.
[22] Barcellona S, Colnago S, Dotelli G, Latorrata S, Piegari L. Aging effect on the variation of Li-ion battery resistance as function of temperature and state of charge. J Energy Storage 2022;50:104658. http://dx.doi.org/10.1016/j.est.2022.104658.
[23] Neupert S, Kowal J. Model-based state-of-charge and state-of-health estimation algorithms utilizing a new free Lithium-Ion battery cell dataset for benchmarking purposes. Batter 2023;9(7):364. http://dx.doi.org/10.3390/batteries9070364.
[24] How DNT, Hannan MA, Hossain Lipu MS, Ker PJ. State of charge estimation for Lithium-Ion batteries using model-based and data-driven methods: A review. IEEE Access 2019;7:136116–36. http://dx.doi.org/10.1109/ACCESS.2019.2942213.
[25] Ren Z, Du C. A review of machine learning state-of-charge and state-of-health estimation algorithms for Lithium-Ion batteries. Energy Rep 2023;9:2993–3021. http://dx.doi.org/10.1016/j.egyr.2023.01.108.
[26] Liu Y, He Y, Bian H, Guo W, Zhang X. A review of Lithium-Ion battery state of charge estimation based on deep learning: Directions for improvement and future trends. J Energy Storage 2022;52:104664. http://dx.doi.org/10.1016/j.est.2022.104664.
[27] Cui Z, Wang L, Li Q, Wang K. A comprehensive review on the state of charge estimation for lithium-ion battery based on neural network. Int J Energy Res 2022;46(5):5423–40. http://dx.doi.org/10.1002/er.7545.
[28] Luo K, Chen X, Zheng H, Shi Z. A review of deep learning approach to predicting the state of health and state of charge of Lithium-Ion batteries. J Energy Chem 2022;74:159–73. http://dx.doi.org/10.1016/j.jechem.2022.06.049.
[29] Baccouche I, Jemmali S, Mlayah A, Manai B, Amara NEB. Implementation of an improved Coulomb-counting algorithm based on a piecewise SOC-OCV relationship for SOC estimation of li-ionbattery. 2018, http://dx.doi.org/10.48550/arXiv.1803.10654, arXiv:1803.10654.
[30] He L, Guo D. An improved Coulomb counting approach based on numerical iteration for SOC estimation with real-time error correction ability. IEEE Access 2019;7:74274–82. http://dx.doi.org/10.1109/ACCESS.2019.2921105.
[31] Pillai P, Sundaresan S, Kumar P, Pattipati KR, Balasingam B. Open-circuit voltage models for battery management systems: A review. Energies 2022;15(18):6803. http://dx.doi.org/10.3390/en15186803.
[32] Sundaresan S, Devabattini B, Kumar P, Pattipati K, Balasingam B. Tabular open circuit voltage modelling of li-ion batteries for robust SOC estimation. Energies 2022;15(23):9142. http://dx.doi.org/10.3390/en15239142.
[33] Rodrigues S, Munichandraiah N, Shukla A. A review of state-of-charge indication of batteries by means of a.c. impedance measurements. J Power Sources 2000;87(1–2):12–20. http://dx.doi.org/10.1016/S0378-7753(99)00351-1.
[34] Wang X, Wei X, Zhu J, Dai H, Zheng Y, Xu X, Chen Q. A review of modeling, acquisition, and application of Lithium-Ion battery impedance for onboard battery management. ETransportation 2021;7:100093. http://dx.doi.org/10.1016/j.etran.2020.100093.
[35] Mc Carthy K, Gullapalli H, Ryan KM, Kennedy T. Review—use of impedance spectroscopy for the estimation of li-ion battery state of charge, state of health and internal temperature. J Electrochem Soc 2021;168(8):080517. http://dx.doi.org/10.1149/1945-7111/ac1a85.
[36] Cuadras A, Kanoun O. SoC Li-ion battery monitoring with impedance spectroscopy. In: 2009 6th international multi-conference on systems, signals and devices. Djerba, Tunisia: IEEE; 2009, p. 1–5. http://dx.doi.org/10.1109/SSD.2009.4956761.

[37] Wang L, Zhao X, Deng Z, Yang L. Application of electrochemical impedance spectroscopy in battery management system: State of charge estimation for aging batteries. J Energy Storage 2023;57:106275. http://dx.doi.org/10.1016/j.est.2022.106275.
[38] Uhm T, Kim S. State-of-charge estimation for remaining flying time prediction of small UAV using adaptive robust extended Kalman filter. IEEE Trans Aerosp Electron Syst 2024;1–20. http://dx.doi.org/10.1109/TAES.2024.3449273.
[39] Naseri F, Schaltz E, Stroe D-I, Gismero A, Farjah E. An enhanced equivalent circuit model with real-time parameter identification for battery state-of-charge estimation. IEEE Trans Ind Electron 2022;69(4):3743–51. http://dx.doi.org/10.1109/TIE.2021.3071679.
[40] Lin X, Tang Y, Ren J, Wei Y. State of charge estimation with the adaptive unscented Kalman filter based on an accurate equivalent circuit model. J Energy Storage 2021;41:102840. http://dx.doi.org/10.1016/j.est.2021.102840.
[41] Liu Y, Ma R, Pang S, Xu L, Zhao D, Wei J, Huangfu Y, Gao F. A nonlinear observer SOC estimation method based on electrochemical model for Lithium-Ion battery. IEEE Trans Ind Appl 2021;57(1):1094–104. http://dx.doi.org/10.1109/TIA.2020.3040140.
[42] Yu Z, Huai R, Xiao L. State-of-charge estimation for Lithium-Ion batteries using a Kalman filter based on local linearization. Energies 2015;8(8):7854–73. http://dx.doi.org/10.3390/en8087854.
[43] Zhao X, Sun B, Zhang W, He X, Ma S, Zhang J, Liu X. Error theory study on EKF-based SOC and effective error estimation strategy for Li-ion batteries. Appl Energy 2024;353:121992. http://dx.doi.org/10.1016/j.apenergy.2023.121992.
[44] Zhang X, Duan L, Gong Q, Wang Y, Song H. State of charge estimation for Lithium-Ion battery based on adaptive extended Kalman filter with improved residual covariance matrix estimator. J Power Sources 2024;589:233758. http://dx.doi.org/10.1016/j.jpowsour.2023.233758.
[45] Zhou Z, Zhan M, Wu B, Xu G, Zhang X, Cheng J, Gao M. A novel adaptive unscented Kalman filter algorithm for SOC estimation to reduce the sensitivity of attenuation coefficient. Energy 2024;307:132598. http://dx.doi.org/10.1016/j.energy.2024.132598.
[46] Wang J, Song J, Li Y, Ren T, Yang Z. State of charge estimation for Lithium-Ion battery based on improved online parameters identification and adaptive square root unscented Kalman filter. J Energy Storage 2024;77:109977. http://dx.doi.org/10.1016/j.est.2023.109977.
[47] Tulsyan A, Tsai Y, Gopaluni RB, Braatz RD. State-of-charge estimation in Lithium-Ion batteries: A particle filter approach. J Power Sources 2016;331:208–23. http://dx.doi.org/10.1016/j.jpowsour.2016.08.113.
[48] Wu T, Liu S, Wang Z, Huang Y. SOC and SOH joint estimation of Lithium-Ion battery based on improved particle filter algorithm. J Electr Eng Technol 2022;17(1):307–17. http://dx.doi.org/10.1007/s42835-021-00861-y.
[49] Hu X, Sun F, Zou Y. Estimation of state of charge of a Lithium-Ion battery pack for electric vehicles using an adaptive luenberger observer. Energies 2010;3(9):1586–603. http://dx.doi.org/10.3390/en3091586.
[50] Hansen T, Wang C-J. Support vector based battery state of charge estimator. J Power Sources 2005;141(2):351–8. http://dx.doi.org/10.1016/j.jpowsour.2004.09.020.
[51] Hu J, Hu J, Lin H, Li X, Jiang C, Qiu X, Li W. State-of-charge estimation for battery management system using optimized support vector machine for regression. J Power Sources 2014;269:682–93. http://dx.doi.org/10.1016/j.jpowsour.2014.07.016.
[52] Saji D, Babu PS, Ilango K. SoC estimation of Lithium Ion battery using combined coulomb counting and fuzzy logic method. In: 2019 4th international conference on recent trends on electronics, information, communication & technology. RTEICT, Bangalore, India: IEEE; 2019, p. 948–52. http://dx.doi.org/10.1109/RTEICT46194.2019.9016956.
[53] Zenati A, Desprez Ph, Razik H. Estimation of the SOC and the SOH of li-ion batteries, by combining impedance measurements with the fuzzy logic inference. In: IECON 2010 - 36th annual conference on IEEE industrial electronics society. Glendale, AZ, USA: IEEE; 2010, p. 1773–8. http://dx.doi.org/10.1109/IECON.2010.5675408.
[54] dos Reis G, Strange C, Yadav M, Li S. Lithium-Ion battery data and where to find it. Energy AI 2021;5:100081. http://dx.doi.org/10.1016/j.egyai.2021.100081.
[55] National Renewable Energy Laboratory. NREL DriveCAT: Drive cycle analysis tool. 2024, https://www.nrel.gov/transportation/drive-cycle-tool.
[56] Yao J, Kowal J. A multi-scale data-driven framework for online state of charge estimation of Lithium-Ion batteries with a novel public drive cycle dataset. J Energy Storage 2025;107:114888. http://dx.doi.org/10.1016/j.est.2024.114888.
[57] Kollmeyer P. Panasonic 18650PF Li-ion battery data. 2018, http://dx.doi.org/10.17632/WYKHT8Y7TG.1.
[58] Chemali E, Kollmeyer PJ, Preindl M, Ahmed R, Emadi A. Long short-term memory networks for accurate state-of-charge estimation of Li-ion batteries. IEEE Trans Ind Electron 2018;65(8):6730–9. http://dx.doi.org/10.1109/TIE.2017.2787586.
[59] Chemali E, Kollmeyer PJ, Preindl M, Emadi A. State-of-charge estimation of Li-ion batteries using deep neural networks: A machine learning approach. J Power Sources 2018;400:242–55. http://dx.doi.org/10.1016/j.jpowsour.2018.06.104.
[60] Bian C, Duan Z, Hao Y, Yang S, Feng J. Exploring large language model for generic and robust state-of-charge estimation of Li-ion batteries: A mixed prompt learning method. Energy 2024;302:131856. http://dx.doi.org/10.1016/j.energy.2024.131856.
[61] Naguib M. LG 18650HG2 Li-ion battery data and example deep neural network xEV SOC estimator script. 2020, http://dx.doi.org/10.17632/CP3473X7XV.3.
[62] Kollmeyer P. Samsung INR21700 30T 3Ah Li-ion battery data. 2023, http://dx.doi.org/10.17632/9XYVY2NJJ3.2.
[63] Yao J. Lithium-ion battery drive cycle dataset. 2024, http://dx.doi.org/10.14279/DEPOSITONCE-21133.
[64] Battery data | Center for advanced life cycle engineering. https://calce.umd.edu/battery-data.
[65] Hannan MA, Lipu MSH, Hussain A, Saad MH, Ayob A. Neural network approach for estimating state of charge of Lithium-Ion battery using backtracking search algorithm. IEEE Access 2018;6:10069–79. http://dx.doi.org/10.1109/ACCESS.2018.2797976.
[66] How DNT, Hannan MA, Lipu MSH, Sahari KSM, Ker PJ, Muttaqi KM. State-of-charge estimation of Li-Ion battery in electric vehicles: A deep neural network approach. IEEE Trans Ind Appl 2020;56(5):5565–74. http://dx.doi.org/10.1109/TIA.2020.3004294.
[67] Lipu MH, Hannan MA, Hussain A, Saad M, Ayob A, Muttaqi KM. Lithium-Ion battery state of charge estimation method using optimized deep recurrent neural network algorithm. In: 2019 IEEE industry applications society annual meeting. Baltimore, MD, USA: IEEE; 2019, p. 1–9. http://dx.doi.org/10.1109/IAS.2019.8912322.
[68] Feng X, Chen J, Zhang Z, Miao S, Zhu Q. State-of-charge estimation of Lithium-Ion battery based on clockwork recurrent neural network. Energy 2021;236:121360. http://dx.doi.org/10.1016/j.energy.2021.121360.
[69] Hochreiter S, Schmidhuber J. Long short-term memory. Neural Comput 1997;9(8):1735–80. http://dx.doi.org/10.1162/neco.1997.9.8.1735.
[70] Yang F, Song X, Xu F, Tsui K-L. State-of-charge estimation of Lithium-Ion batteries via long short-term memory network. IEEE Access 2019;7:53792–9. http://dx.doi.org/10.1109/ACCESS.2019.2912803.
[71] Bian C, He H, Yang S. Stacked bidirectional long short-term memory networks for state-of-charge estimation of Lithium-Ion batteries. Energy 2020;191:116538. http://dx.doi.org/10.1016/j.energy.2019.116538.
[72] Chen J, Zhang Y, Wu J, Cheng W, Zhu Q. SOC estimation for Lithium-Ion battery using the LSTM-RNN with extended input and constrained output. Energy 2023;262:125375. http://dx.doi.org/10.1016/j.energy.2022.125375.
[73] Jiao M, Wang D. The Savitzky-Golay filter based bidirectional long short-term memory network for SOC estimation. Int J Energy Res 2021;45(13):19467–80. http://dx.doi.org/10.1002/er.7055.
[74] Li C, Xiao F, Fan Y, Yang G, Zhang W. A recurrent neural network with long short-term memory for state of charge estimation of Lithium-ion batteries. In: 2019 IEEE 8th joint international information technology and artificial intelligence conference. ITAIC, Chongqing, China: IEEE; 2019, p. 1712–6. http://dx.doi.org/10.1109/ITAIC.2019.8785770.
[75] Fasahat M, Manthouri M. State of charge estimation of Lithium-Ion batteries using hybrid autoencoder and long short term memory neural networks. J Power Sources 2020;469:228375. http://dx.doi.org/10.1016/j.jpowsour.2020.228375.
[76] Cho K, van Merrienboer B, Gulcehre C, Bahdanau D, Bougares F, Schwenk H, Bengio Y. Learning phrase representations using RNN encoder-decoder for statistical machine translation. 2014, http://dx.doi.org/10.48550/ARXIV.1406.1078.
[77] Yang F, Li W, Li C, Miao Q. State-of-charge estimation of Lithium-Ion batteries based on gated recurrent neural network. Energy 2019;175:66–75. http://dx.doi.org/10.1016/j.energy.2019.03.059.
[78] Li C, Xiao F, Fan Y. An approach to state of charge estimation of Lithium-Ion batteries based on recurrent neural networks with gated recurrent unit. Energies 2019;12(9):1592. http://dx.doi.org/10.3390/en12091592.
[79] Hannan MA, How DNT, Mansor M, Lipu MSH, Ker PJ, Muttaqi KM. State-of-charge estimation of Li-ion battery at variable ambient temperature with gated recurrent unit network. In: 2020 IEEE industry applications society annual meeting. Detroit, MI, USA: IEEE; 2020, p. 1–8. http://dx.doi.org/10.1109/IAS44978.2020.9334824.
[80] Duan W, Song C, Peng S, Xiao F, Shao Y, Song S. An improved gated recurrent unit network model for state-of-charge estimation of Lithium-Ion battery. Energies 2020;13(23):6366. http://dx.doi.org/10.3390/en13236366.
[81] Zhang Z, Dong Z, Lin H, He Z, Wang M, He Y, Gao X, Gao M. An improved bidirectional gated recurrent unit method for accurate state-of-charge estimation. IEEE Access 2021;9:11252–63. http://dx.doi.org/10.1109/ACCESS.2021.3049944.
[82] Chen J, Feng X, Jiang L, Zhu Q. State of charge estimation of Lithium-Ion battery using denoising autoencoder and gated recurrent unit recurrent neural network. Energy 2021;227:120451. http://dx.doi.org/10.1016/j.energy.2021.120451.
[83] Bhattacharjee A, Verma A, Mishra S, Saha TK. Estimating state of charge for xEV batteries using 1D convolutional neural networks and transfer learning. IEEE Trans Veh Technol 2021;70(4):3123–35. http://dx.doi.org/10.1109/TVT.2021.3064287.

[84] Fan X, Zhang W, Zhang C, Chen A, An F. SOC estimation of Li-ion battery using convolutional neural network with U-Net architecture. Energy 2022;256:124612. http://dx.doi.org/10.1016/j.energy.2022.124612.

[85] Kim K-H, Oh K-H, Ahn H-S, Choi H-D. Time–frequency domain deep convolutional neural network for Li-Ion battery SoC estimation. IEEE Trans Power Electron 2024;39(1):125–34. http://dx.doi.org/10.1109/TPEL.2023.3309934.

[86] Bai S, Kolter JZ, Koltun V. An empirical evaluation of generic convolutional and recurrent networks for sequence modeling. 2018, http://dx.doi.org/10.48550/arXiv.1803.01271, arXiv:1803.01271.

[87] Liu Y, Li J, Zhang G, Hua B, Xiong N. State of charge estimation of Lithium-Ion batteries based on temporal convolutional network and transfer learning. IEEE Access 2021;9:34177–87. http://dx.doi.org/10.1109/ACCESS.2021.3057371.

[88] Mohan NC, Priyadarshi H, Patidar VK, Panigrahi BK, Saxena S. Battery state of charge estimation with separable temporal convolutional networks. In: 2024 IEEE 4th international conference on sustainable energy and future electric transportation. SEFET, Hyderabad, India: IEEE; 2024, p. 1–6. http://dx.doi.org/10.1109/SEFET61574.2024.10717918.

[89] Yu T, Zhu H. Hyper-parameter optimization: A review of algorithms and applications. 2020, http://dx.doi.org/10.48550/arXiv.2003.05689, arXiv:2003.05689.

[90] Yang B, Wang Y, Zhan Y. Lithium battery state-of-charge estimation based on a Bayesian optimization bidirectional long short-term memory neural network. Energies 2022;15(13):4670. http://dx.doi.org/10.3390/en15134670.

[91] How DNT, Hannan MA, Lipu MSH, Ker PJ, Mansor M, Sahari KSM, Muttaqi KM. SOC estimation using deep bidirectional gated recurrent units with tree parzen estimator hyperparameter optimization. IEEE Trans Ind Appl 2022;58(5):6629–38. http://dx.doi.org/10.1109/TIA.2022.3180282.

[92] Chen J, Lu C, Chen C, Cheng H, Xuan D. An improved gated recurrent unit neural network for state-of-charge estimation of Lithium-Ion battery. Appl Sci 2022;12(5):2305. http://dx.doi.org/10.3390/app12052305.

[93] Chai X, Li S, Liang F. A novel battery SOC estimation method based on random search optimized LSTM neural network. Energy 2024;306:132583. http://dx.doi.org/10.1016/j.energy.2024.132583.

[94] Bahdanau D, Cho K, Bengio Y. Neural machine translation by jointly learning to align and translate. 2016, http://dx.doi.org/10.48550/arXiv.1409.0473, arXiv:1409.0473.

[95] Vaswani A, Shazeer N, Parmar N, Uszkoreit J, Jones L, Gomez AN, Kaiser L, Polosukhin I. Attention is all you need. 2023, http://dx.doi.org/10.48550/arXiv.1706.03762, arXiv:1706.03762.

[96] Yang K, Tang Y, Zhang S, Zhang Z. A deep learning approach to state of charge estimation of Lithium-Ion batteries based on dual-stage attention mechanism. Energy 2022;244:123233. http://dx.doi.org/10.1016/j.energy.2022.123233.

[97] Yang K, Wang Y, Tang Y, Zhang S, Zhang Z. A temporal convolution and gated recurrent unit network with attention for state of charge estimation of Lithium-Ion batteries. J Energy Storage 2023;72:108774. http://dx.doi.org/10.1016/j.est.2023.108774.

[98] Mamo T, Wang F-K. Long short-term memory with attention mechanism for state of charge estimation of Lithium-Ion batteries. IEEE Access 2020;8:94140–51. http://dx.doi.org/10.1109/ACCESS.2020.2995656.

[99] Han Y, Liu Y, Huang Q, Zhang Y. SOC estimation for Lithium-Ion batteries based on BiGRU with SE attention and Savitzky-Golay filter. J Energy Storage 2024;90:111930. http://dx.doi.org/10.1016/j.est.2024.111930.

[100] Song Y, Park S, Kim SW, Koo G. Self-attention network-based state of charge estimation for Lithium-Ion batteries with gapped temperature data. Expert Syst Appl 2025;261:125498. http://dx.doi.org/10.1016/j.eswa.2024.125498.

[101] Wu L, Zhang Y. Attention-based encoder-decoder networks for state of charge estimation of Lithium-Ion battery. Energy 2023;268:126665. http://dx.doi.org/10.1016/j.energy.2023.126665.

[102] Zhuang F, Qi Z, Duan K, Xi D, Zhu Y, Zhu H, Xiong H, He Q. A comprehensive survey on transfer learning. 2020, http://dx.doi.org/10.48550/arXiv.1911.02685, arXiv:1911.02685.

[103] Vidal C, Kollmeyer P, Chemali E, Emadi A. Li-ion battery state of charge estimation using long short-term memory recurrent neural network with transfer learning. In: 2019 IEEE transportation electrification conference and expo. ITEC, Detroit, MI, USA: IEEE; 2019, p. 1–6. http://dx.doi.org/10.1109/ITEC.2019.8790543.

[104] Qin Y, Adams S, Yuen C. Transfer learning-based state of charge estimation for Lithium-Ion battery at varying ambient temperatures. IEEE Trans Ind Inform 2021;17(11):7304–15. http://dx.doi.org/10.1109/TII.2021.3051048.

[105] Oyewole I, Chehade A, Kim Y. A controllable deep transfer learning network with multiple domain adaptation for battery state-of-charge estimation. Appl Energy 2022;312:118726. http://dx.doi.org/10.1016/j.apenergy.2022.118726.

[106] Eleftheriadis P, Giazitzis S, Leva S, Ogliari E. Transfer learning techniques for the Lithium-Ion battery state of charge estimation. IEEE Access 2024;12:993–1004. http://dx.doi.org/10.1109/ACCESS.2023.3337215.

[107] Xu H, Xu Q, Duanmu F, Shen J, Jin L, Gou B, Wu F, Zhang W. State-of-charge estimation of Lithium-Ion batteries based on EKF integrated with PSO-LSTM for electric vehicles. IEEE Trans Transp Electr 2025;11(1):2311–21. http://dx.doi.org/10.1109/TTE.2024.3421260.

[108] Yang F, Zhang S, Li W, Miao Q. State-of-charge estimation of Lithium-Ion batteries using LSTM and UKF. Energy 2020;201:117664. http://dx.doi.org/10.1016/j.energy.2020.117664.

[109] Yu Z, Liu J, Lu Y, Feng C, Li L, Wu Q. Combined EKF–LSTM algorithm-based enhanced state-of-charge estimation for energy storage container cells. J Power Electron 2024;24(8):1329–39. http://dx.doi.org/10.1007/s43236-024-00801-9.

[110] He W, Ma H, Guo R, Xu J, Xie Z, Wen H. Enhancing the state-of-charge estimation of Lithium-Ion batteries using a CNN-BiGRU and AUKF fusion model. Comput Electr Eng 2024;120:109729. http://dx.doi.org/10.1016/j.compeleceng.2024.109729.

[111] Yu H, Lu H, Zhang Z, Yang L. A generic fusion framework integrating deep learning and Kalman filter for state of charge estimation of Lithium-Ion batteries: Analysis and comparison. J Power Sources 2024;623:235493. http://dx.doi.org/10.1016/j.jpowsour.2024.235493.

[112] Yao J, Neupert S, Kowal J. Cross-stitch networks for joint state of charge and state of health online estimation of Lithium-Ion batteries. Batteries 2024;10(6):171. http://dx.doi.org/10.3390/batteries10060171.

[113] Krzywanski J, Sosnowski M, Grabowska K, Zylka A, Lasek L, Kijo-Kleczkowska A. Advanced computational methods for modeling, prediction and optimization—A review. Mater 2024;17(14):3521. http://dx.doi.org/10.3390/ma17143521.

[114] Krzywanski J, Skrobek D, Sosnowski M, Ashraf WM, Grabowska K, Zylka A, Kulakowska A, Nowak W, Sztekler K, Shahzad MW. Towards enhanced heat and mass exchange in adsorption systems: The role of AutoML and fluidized bed innovations. Int Commun Heat Mass Transfer 2024;152:107262. http://dx.doi.org/10.1016/j.icheatmasstransfer.2024.107262.

[115] Krzywanski J, Sztekler K, Lasek L, Kalawa W, Grabowska K, Sosnowski M, Zylka A, Skrobek D, Nowak W, Shboul B. Performance enhancement of adsorption cooling and desalination systems by fluidized bed integration: Experimental and big data optimization. Energy 2025;315:134347. http://dx.doi.org/10.1016/j.energy.2024.134347.

[116] Witvoet K, Saad S, Vidal C, Ahmed R, Emadi A. Electric vehicle's range and state of charge estimations using AutoML. In: 2023 IEEE transportation electrification conference & expo. ITEC, Detroit, MI, USA: IEEE; 2023, p. 1–6. http://dx.doi.org/10.1109/ITEC55900.2023.10186953.

[117] Yao J, Zheng B, Kowal J. Continual learning for online state of charge estimation across diverse Lithium-Ion batteries. J Energy Storage 2025;117:116086. http://dx.doi.org/10.1016/j.est.2025.116086.

[118] Raissi M, Perdikaris P, Karniadakis G. Physics-informed neural networks: A deep learning framework for solving forward and inverse problems involving nonlinear partial differential equations. J Comput Phys 2019;378:686–707. http://dx.doi.org/10.1016/j.jcp.2018.10.045.

[119] Singh S, Ebongue YE, Rezaei S, Birke KP. Hybrid modeling of Lithium-Ion battery: Physics-informed neural network for battery state estimation. Batter 2023;9(6):301. http://dx.doi.org/10.3390/batteries9060301.

[120] Tian A, He L, Dong K, Ding T, Gao Y, Jiang J, Yang X. An extended single-particle model based on physics-informed neural network for SOC state estimation of Lithium-Ion batteries. In: Li K, Liu K, Hu Y, Tan M, Zhang L, Yang Z, editors. Clean energy technology and energy storage systems. vol. 2218, Singapore: Springer Nature Singapore; 2025, p. 300–16. http://dx.doi.org/10.1007/978-981-96-0232-2_24.

[121] Baraean A, Kassas M, Abido M. Physics-informed NN for improving electric vehicles Lithium-Ion battery state-of-charge estimation robustness. In: 2024 IEEE 12th international conference on smart energy grid engineering. SEGE, Oshawa, ON, Canada: IEEE; 2024, p. 245–50. http://dx.doi.org/10.1109/SEGE62220.2024.10739432.

[122] P A, R SV, Cephas I. Physics informed neural networks for reliable SOC estimation in Lithium-Ion battery management. In: 2024 9th international conference on communication and electronics systems. ICCES, Coimbatore, India: IEEE; 2024, p. 41–7. http://dx.doi.org/10.1109/ICCES63552.2024.10860002.

[123] Wang Y, Han X, Guo D, Lu L, Chen Y, Ouyang M. Physics-informed recurrent neural network with fractional-order gradients for state-of-charge estimation of Lithium-Ion battery. IEEE J Radio Freq Identif 2022;6:968–71. http://dx.doi.org/10.1109/JRFID.2022.3211841.

[124] Tian J, Xiong R, Lu J, Chen C, Shen W. Battery state-of-charge estimation amid dynamic usage with physics-informed deep learning. Energy Storage Mater 2022;50:718–29. http://dx.doi.org/10.1016/j.ensm.2022.06.007.

[125] Ruder S. An overview of multi-task learning in deep neural networks. 2017, http://dx.doi.org/10.48550/ARXIV.1706.05098.

[126] Zhang Y, Yang Q. A survey on multi-task learning. IEEE Trans Knowl Data Eng 2022;34(12):5586–609. http://dx.doi.org/10.1109/TKDE.2021.3070203.

[127] Misra I, Shrivastava A, Gupta A, Hebert M. Cross-stitch networks for multi-task learning. 2016, http://dx.doi.org/10.48550/ARXIV.1604.03539.

[128] Ruder S, Bingel J, Augenstein I, Søgaard A. Latent multi-task architecture learning. 2017, http://dx.doi.org/10.48550/ARXIV.1705.08142.

[129] Ma J, Zhao Z, Yi X, Chen J, Hong L, Chi EH. Modeling task relationships in multi-task learning with multi-gate mixture-of-experts. In: Proceedings of the 24th ACM SIGKDD international conference on knowledge discovery & data mining. London United Kingdom: ACM; 2018, p. 1930–9. http://dx.doi.org/10.1145/3219819.3220007.

[130] Bao X, Liu Y, Liu B, Liu H, Wang Y. Multi-state online estimation of Lithium-Ion batteries based on multi-task learning. Energies 2023;16(7):3002. http://dx.doi.org/10.3390/en16073002.

[131] Liu S, Johns E, Davison AJ. End-to-end multi-task learning with attention. 2018, http://dx.doi.org/10.48550/ARXIV.1803.10704.

[132] Che Y, Zheng Y, Wu Y, Lin X, Li J, Hu X, Teodorescu R. Battery states monitoring for electric vehicles based on transferred multi-task learning. IEEE Trans Veh Technol 2023;72(8):10037–47. http://dx.doi.org/10.1109/TVT.2023.3260466.

[133] Bao Z, Nie J, Lin H, Li Z, Gao K, He Z, Gao M. Dual-task learning for joint state-of-charge and state-of-energy estimation of Lithium-Ion battery in electric vehicle. IEEE Trans Transp Electr 2025;11(1):558–69. http://dx.doi.org/10.1109/TTE.2024.3393477.

[134] Song Y, Wang T, Mondal SK, Sahoo JP. A comprehensive survey of few-shot learning: Evolution, applications, challenges, and opportunities. 2022, http://dx.doi.org/10.48550/ARXIV.2205.06743.

[135] Wang Y, Yao Q, Kwok J, Ni LM. Generalizing from a few examples: A survey on few-shot learning. 2019, http://dx.doi.org/10.48550/ARXIV.1904.05046.

[136] Finn C, Abbeel P, Levine S. Model-agnostic meta-learning for fast adaptation of deep networks. 2017, http://dx.doi.org/10.48550/ARXIV.1703.03400.

[137] Koch G, Zemel R, Salakhutdinov R. Siamese neural networks for one-shot image recognition. In: ICML deep learning workshop. vol. 2, 2015.

[138] Vinyals O, Blundell C, Lillicrap T, Kavukcuoglu K, Wierstra D. Matching networks for one shot learning. 2016, http://dx.doi.org/10.48550/ARXIV.1606.04080.

[139] Snell J, Swersky K, Zemel RS. Prototypical networks for few-shot learning. 2017, http://dx.doi.org/10.48550/ARXIV.1703.05175.

[140] Jeong D, Bae S. Estimating battery state-of-charge with a few target training data by meta-learning. J Power Sources 2023;553:232238. http://dx.doi.org/10.1016/j.jpowsour.2022.232238.

[141] Wang Y, Wang L, Li M, Chen Z. A review of key issues for control and management in battery and ultra-capacitor hybrid energy storage systems. ETransportation 2020;4:100064. http://dx.doi.org/10.1016/j.etran.2020.100064.

[142] Yao S, Wang G, Zhu H, Chen Q, Zheng Y. Equalization method of 'LiCoxNiyMn1-x-yO2 - LiFePO4' hybrid battery pack based on charging electric quantity estimation. J Energy Storage 2023;69:107959. http://dx.doi.org/10.1016/j.est.2023.107959.

[143] Naseri F, Barbu C, Sarikurt T. Optimal sizing of hybrid high-energy/high-power battery energy storage systems to improve battery cycle life and charging power in electric vehicle applications. J Energy Storage 2022;55:105768. http://dx.doi.org/10.1016/j.est.2022.105768.

[144] Cheng X, Liu X, Deng H, Lu J, Yu Q. State of charge estimation of LiFePO4 battery in AB hybrid battery packs. J Energy Storage 2025;108:115070. http://dx.doi.org/10.1016/j.est.2024.115070.

[145] McCloskey M, Cohen NJ. Catastrophic interference in connectionist networks: The sequential learning problem. In: Psychology of learning and motivation. vol. 24, Elsevier; 1989, p. 109–65. http://dx.doi.org/10.1016/S0079-7421(08)60536-8.

[146] Hadsell R, Rao D, Rusu AA, Pascanu R. Embracing change: Continual learning in deep neural networks. Trends Cogn Sci 2020;24(12):1028–40. http://dx.doi.org/10.1016/j.tics.2020.09.004.

[147] Aleixo EL, Colonna JG, Cristo M, Fernandes E. Catastrophic forgetting in deep learning: A comprehensive taxonomy. 2023, http://dx.doi.org/10.48550/ARXIV.2312.10549.

[148] Delange M, Aljundi R, Masana M, Parisot S, Jia X, Leonardis A, Slabaugh G, Tuytelaars T. A continual learning survey: Defying forgetting in classification tasks. IEEE Trans Pattern Anal Mach Intell 2021. http://dx.doi.org/10.1109/TPAMI.2021.3057446, 1–1.

[149] Lee M, Kim S, Kim S, Choi J-I. Bilevel-optimized continual learning for predicting capacity degradation of Lithium-Ion batteries. J Energy Storage 2024;86:111187. http://dx.doi.org/10.1016/j.est.2024.111187.

[150] Che Y, Zheng Y, Onori S, Hu X, Teodorescu R. Increasing generalization capability of battery health estimation using continual learning. Cell Rep Phys Sci 2023;4(12):101743. http://dx.doi.org/10.1016/j.xcrp.2023.101743.